Data reduction, calibration, and stellar diameter results using VINCI

J. Meisner

These are (more or less) the original slides from my presentation at Ringberg. I have added these little notes for the benefit of the person reading this presentation posted on the internet.

If you have feedback or questions, you may email me at:
meisner@strw.leidenuniv.nl

Note: The talk I am giving today is really two separate talks. These are the themes addressed in the first part:

- Coherent Integration Methods;
- Measurement of visibility phase and effects of dispersion
- Examples from VINCI and early results from MIDI.

And in the second part:

- Cross-calibration of VINCI data and solving for diameters
- Examples of results from VINCI

Jeff Meisner
Leiden Observatory

First I describe and briefly discuss interferometric data reduction methods and their characteristics. This includes:

Incoherent integration of fringe visibility

Coherent integration

Coherent integration with dispersion tracking

"Quasi-coherent" integration

In some cases I show implementations of these methods both for delay-scanned interferometry and for spectrally-dispersed interferometric detection.

Incoherent, coherent and quasi-coherent integration

Incoherent integration

- No attempt to find the atmospheric OPD
- Treats signal as additional noise source (perhaps with a particular spectral content)
- Result dependent on subtraction of assumed noise level

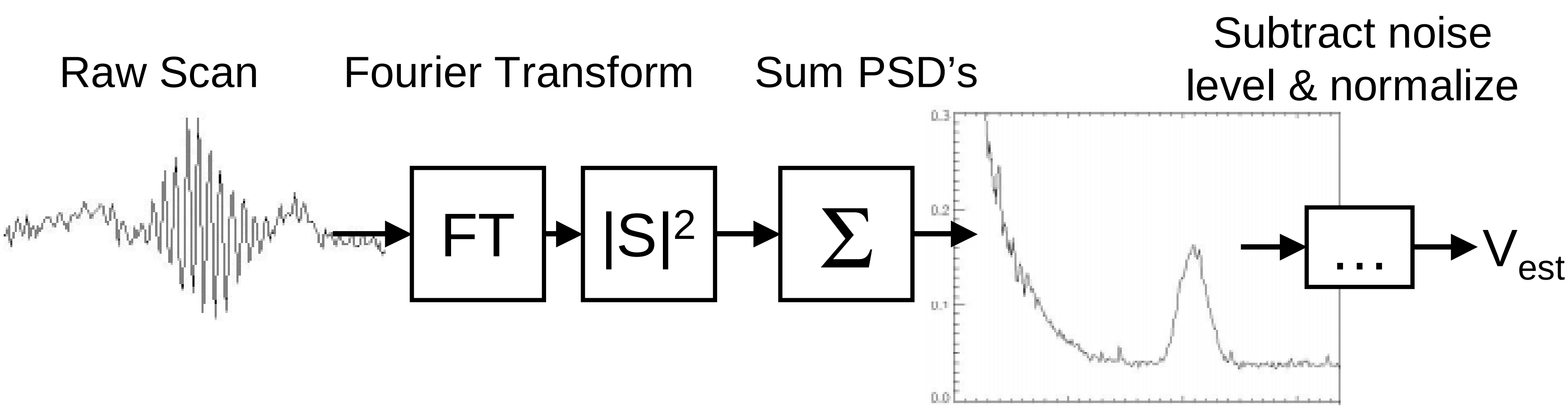

Incoherent, coherent and quasi-coherent integration

Coherent integration

- Use the data (possibly from a different source) itself to estimate the atmospheric OPD τ
- Uses the estimate of τ to correct the data
- Integrate the corrected data to obtain an average

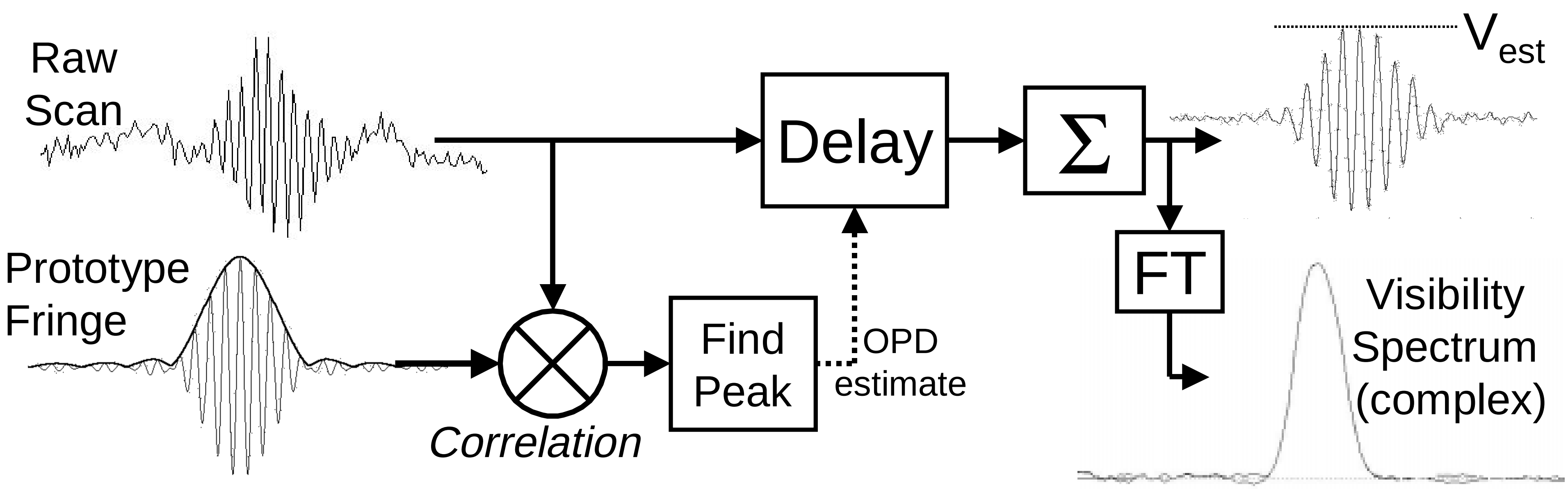

Coherent integration using spectrally dispersed detection. Assumes little or no random dispersion.

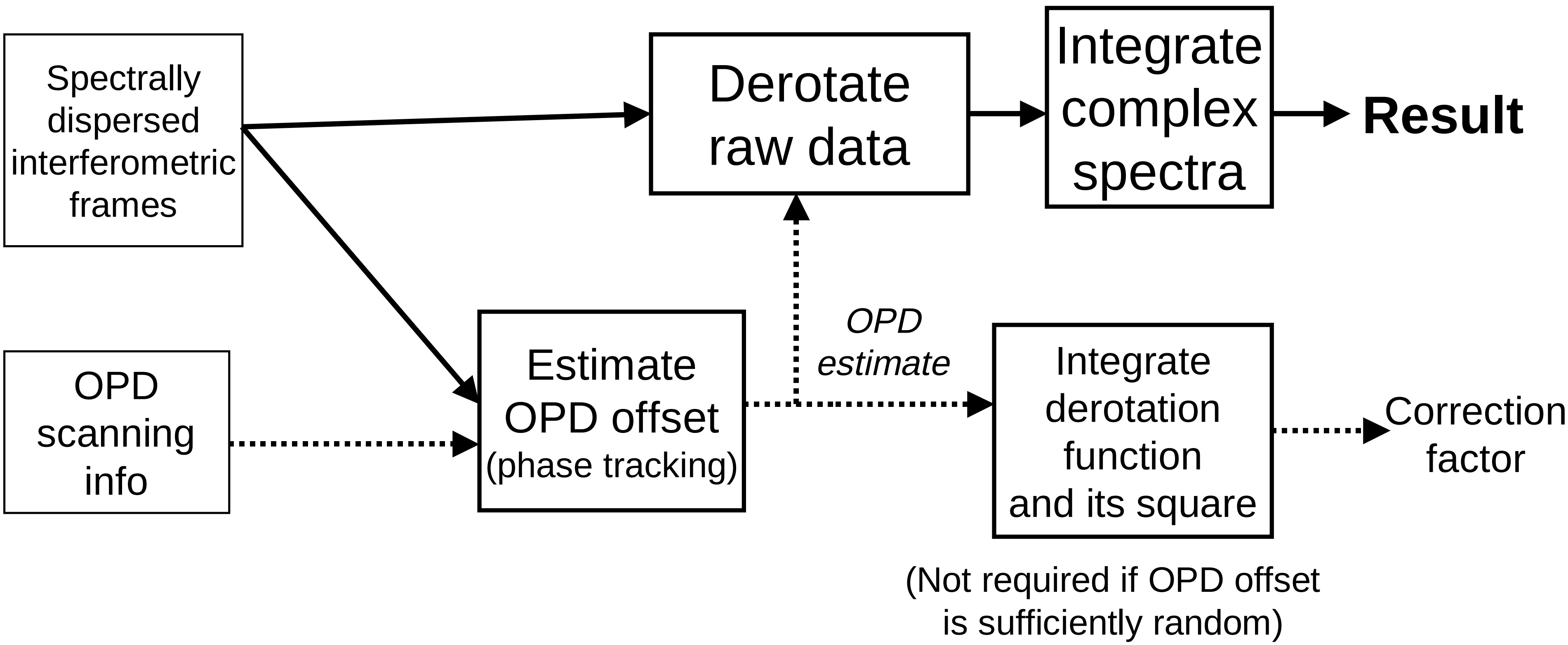

Note that coherent integration, as shown, is an unacceptable solution at most wavelengths under normal conditions, because it does not account for the effects of random dispersion fluctuations due to atmospheric water vapor inhomogeneities.

Coherent integration with a "dispersion tracker" as shown in the next slide solves this problem.

Coherent integration using spectrally dispersed detection *with dispersion tracking*

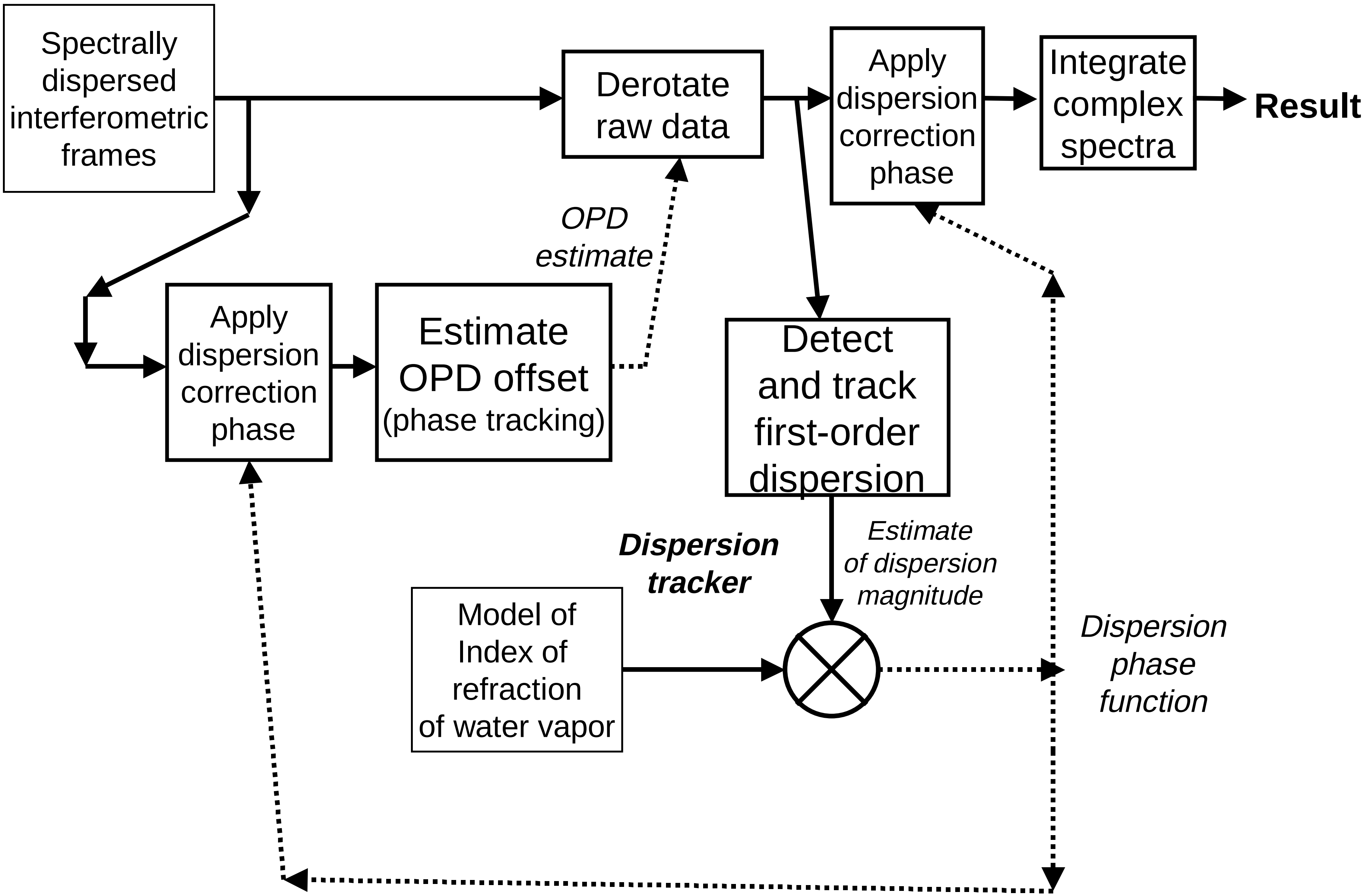

"Quasi-coherent" integration

Similar to coherent integration, except:

- Uses the *group delay* estimator to shift the signal by a large amount
- Applies an additional *phase shift* as a proxy for the remaining required OPD correction to ensure coherence
- Therefore applies a frequency-dependent time shift of $\tau_G + \phi/\nu$ instead of $\tau_G + \phi/\nu_0$
- Very practical for data from medium-narrow bandwidth instruments.

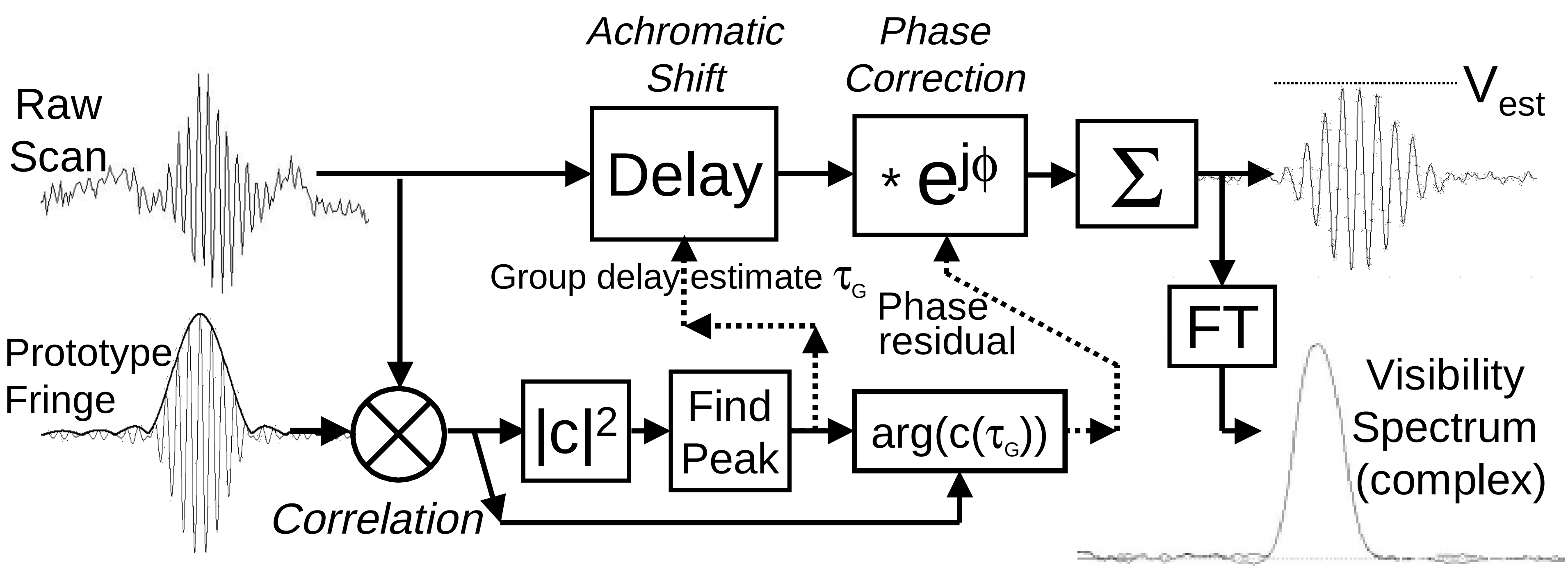

”Quasi-coherent” integration using spectrally dispersed detection.

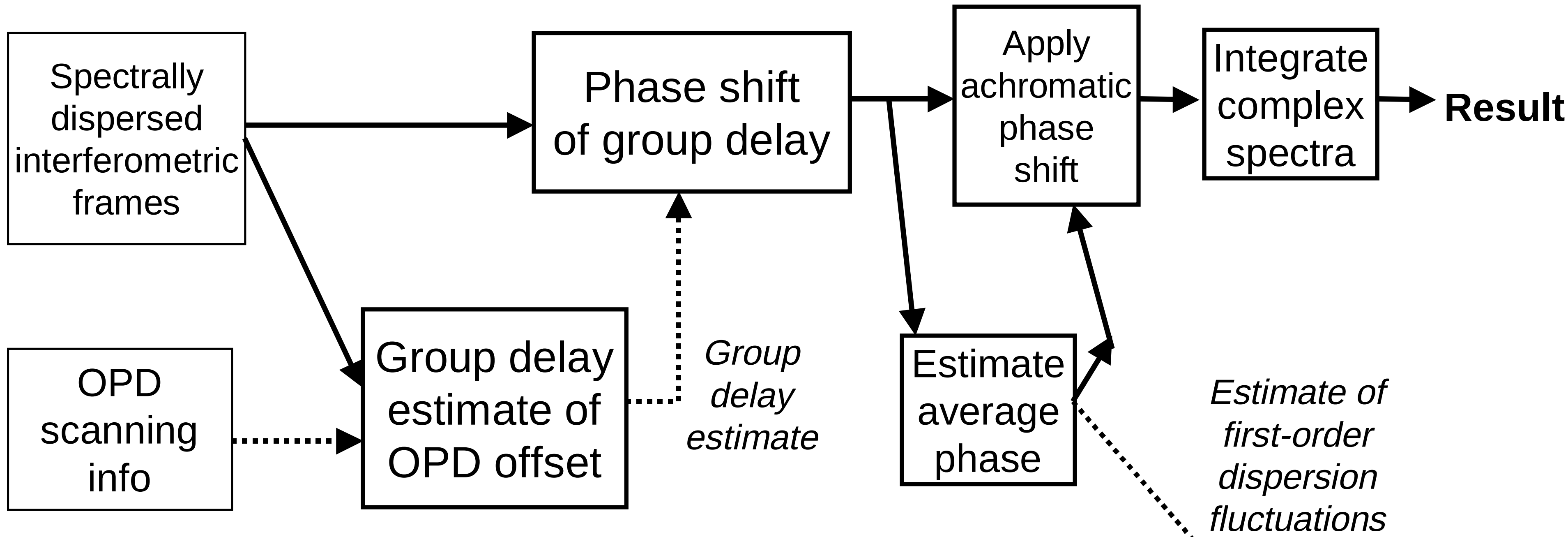

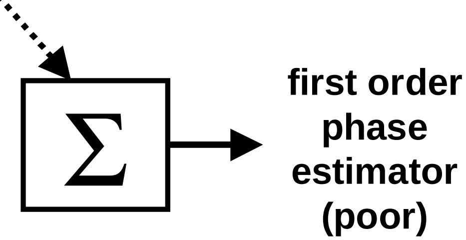

The “quasi-coherent” method shown in these two slides is an alternative solution to dispersion fluctuations. It is simpler (and less model dependent) than a dispersion tracker which models the index of refraction of water vapor in detail. Instead it treats dispersion as being constant in phase across the entire band. Each scan or frame is treated independently rather than using a “tracking” algorithm which expects continuity in the dispersion time series. However it is very adaquate in many situations, such as with the medium-narrowband VINCI data I have reduced.

Disadvantage of quasi-coherent approach:

With wide bandwidth and substantial dispersion fluctuations, there will be a reduction in the visibility spectrum toward the band edges

Dispersion RMS	20 THz (15 μm)	24 THz (12.5 μm)	30 THz (10 μm)	36 THz (8.3 μm)	40 THz (7.5 μm)
1 radian	.95	.98	1.00	.98	.95
2 radians	.80	.92	1.00	.92	.80
3 radians	.61	.83	1.00	.83	.61

This slide shows the reduction in visibility estimates at the edges of the N band due to using the quasi-coherent method, as a function of different amounts of random dispersion fluctuations. The next slide shows that in one particular case where this was measured, the rms of atmospheric dispersion fluctuations (at 10 microns) was found to be 1.65 radians.

Actual water-vapor dispersion fluctuations measured with VLTI instruments.

K band dispersion using VINCI on 16 meter baseline. Dispersion phase Φ_{GD} in degrees over 100 second run with error bars. Full range of graph = 150 degrees = 2.2 moles/m^2 H_2O

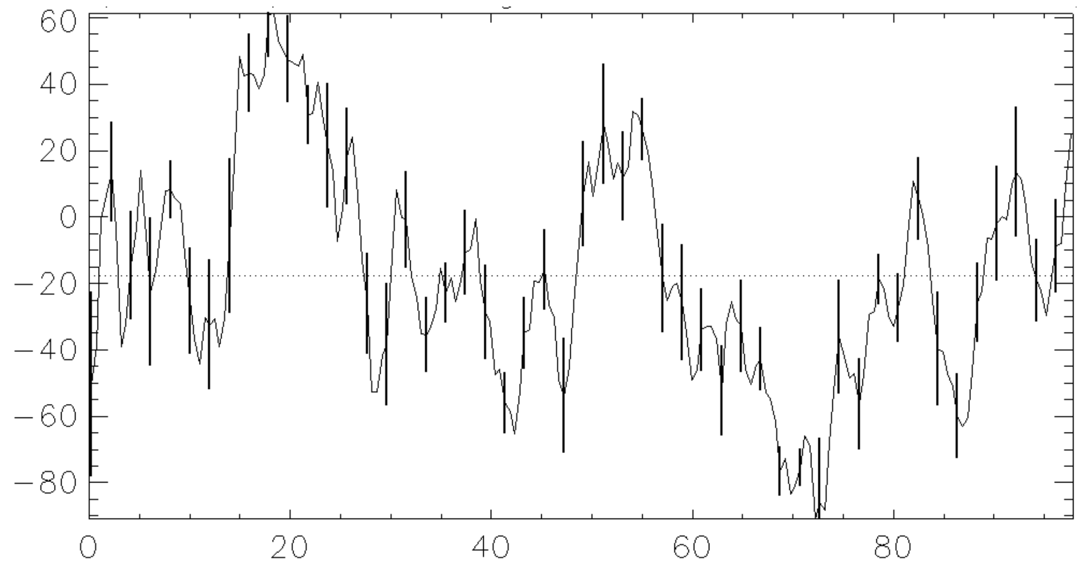

N band dispersion using MIDI, courtesy Walter Jaffe. Dispersion phase Φ_{GD} in degrees over 170 seconds Full range of graph = 10 radians = 4 moles/m^2 H_2O. RMS level = 1.65 = .66 moles/m^2 H_2O

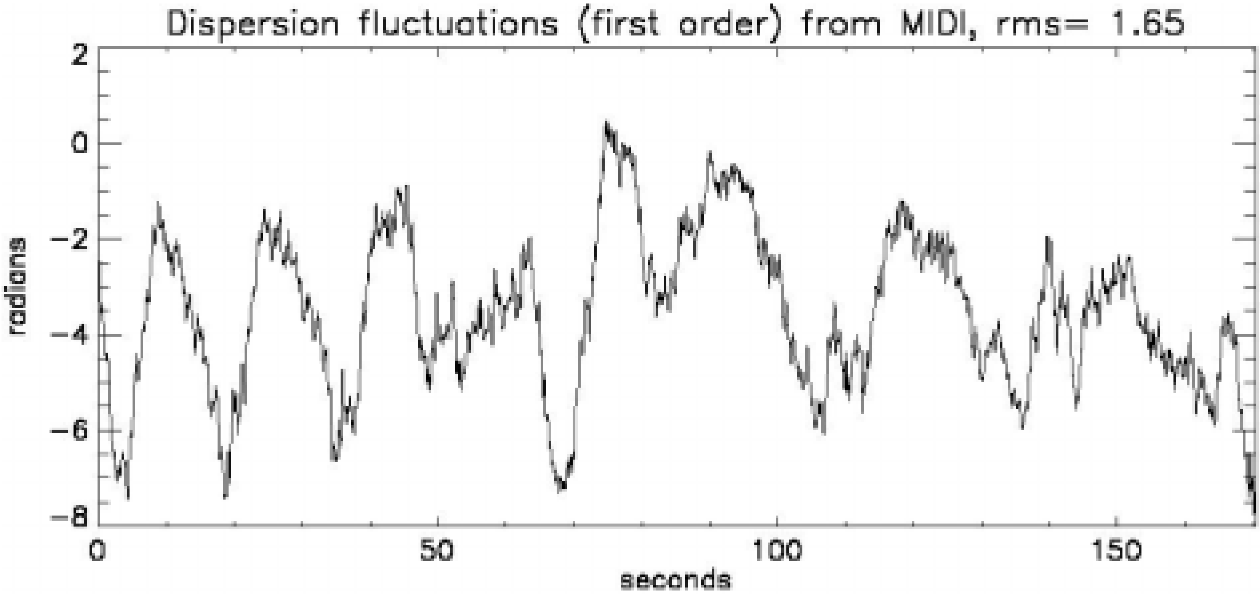

Actual water-vapor dispersion fluctuations measured with MIDI: Power spectrum

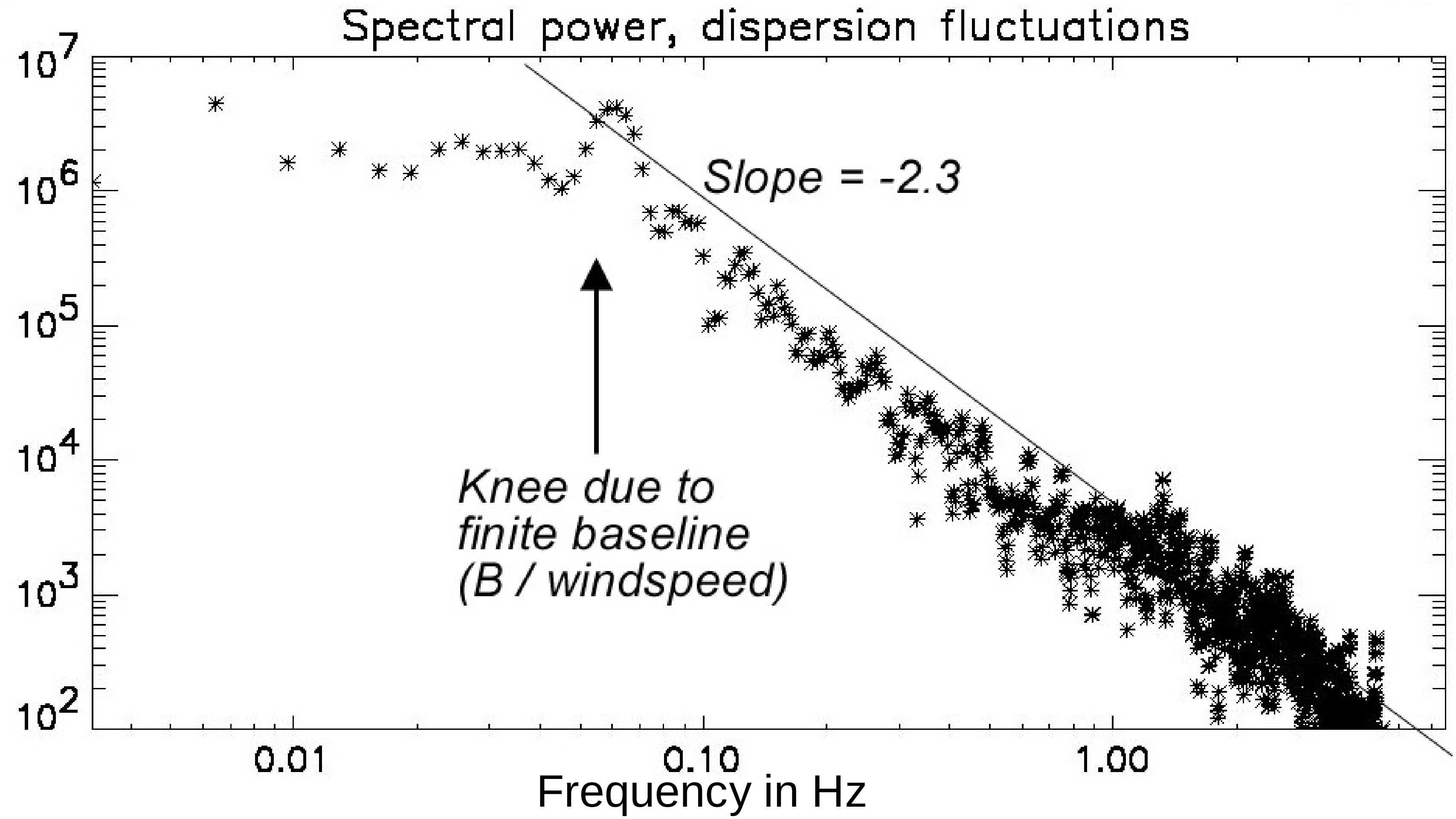

Random walk: slope=2

Kolmogorov process: slope=2.67

Calibrating out instrumental dispersion (including air paths) for detection of true source phase

Method:

Excess air path = **D**

Air dispersion = $\mathbf{d\phi_A/dl}$

Beamcombiner phase = ϕ_B

Measured phase of visibility = ϕ_{RAW}

Then the *corrected* phase for an observation is found as:

$$\phi_{CORR} = \phi_{RAW} - \phi_B - (d\phi_A/dl)\, D$$

This is just showing 2nd (and higher) order dispersion, from a VINCI observation. The quasi-coherent estimator has removed the first order component of the phase function (which will always be difficult/impossible to detect on a source, due to water vapor fluctuations).

Example:

Observation of Sirius, JD2200.36409

UNCORRECTED PHASE:

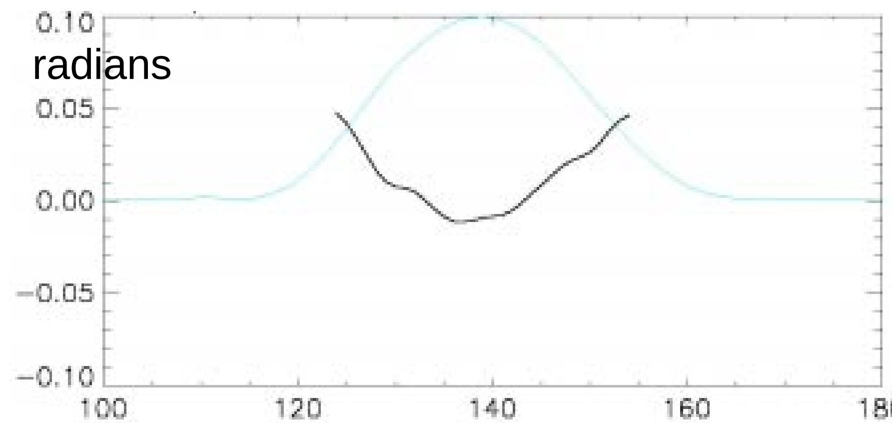

CORRECTED PHASE:

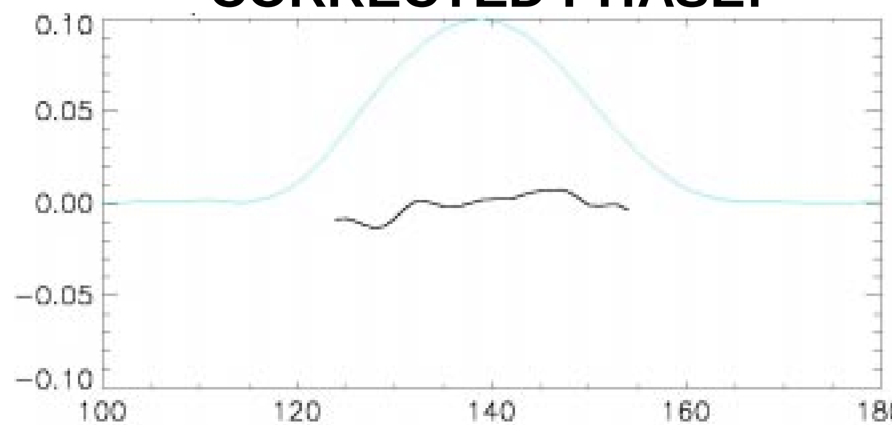

Optical frequency in Tera-Hertz

Measurement of 1st order dispersion (group-delay offset phase) of astronomical sources (??)

First Order Dispersion:

- Inherently difficult to measure with a medium/narrow-band interferometer
- Automatically cancelled using quasi-coherent integration (but can be estimated by averaging the phase residuals)
- Even with the brightest sources, only measurable with about .2 radian rms using VINCI (25% bandwidth). Water vapor dispersion is major noise source
- Must first subtract air dispersion as a function of delay-line position:

Therefore we consider it unfeasible to detect planets (from the ground) by measuring a 1st order dispersion phase offset of ~.001 radian.

However large phase offsets can still be detected (after subtracting air and instrumental dispersion).

What happened in this observation of a very bright M giant?

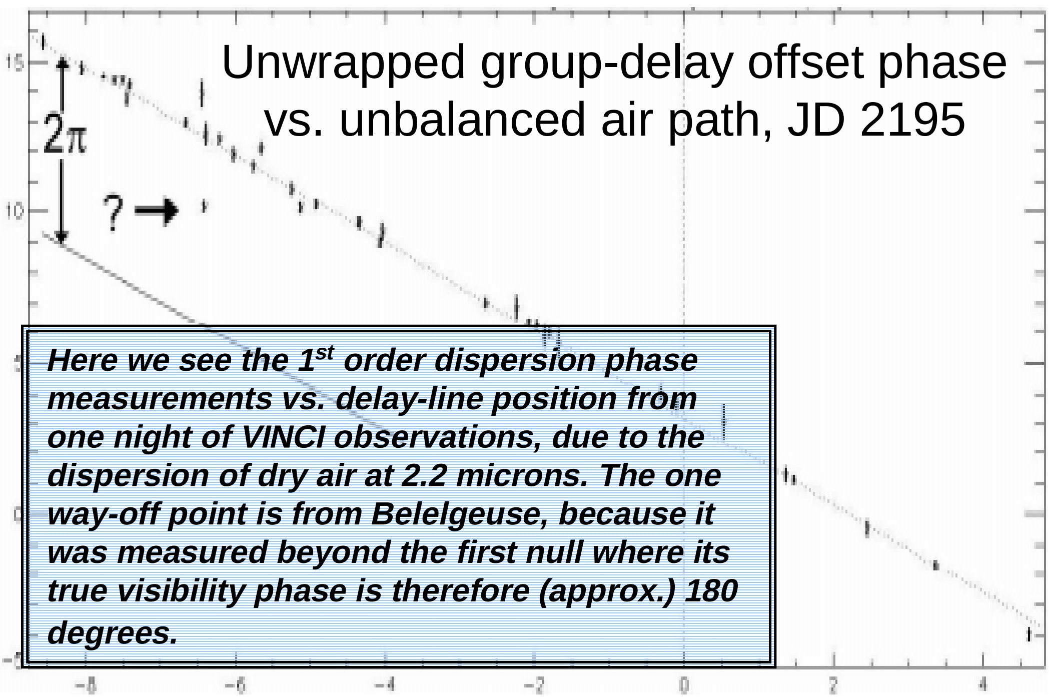

Unwrapped group-delay offset phase vs. unbalanced air path, JD 2195

Here we see the 1st order dispersion phase measurements vs. delay-line position from one night of VINCI observations, due to the dispersion of dry air at 2.2 microns. The one way-off point is from Belelgeuse, because it was measured beyond the first null where its true visibility phase is therefore (approx.) 180 degrees.

Measurement of stellar diameters by observing the null in the coherently integrated visibility spectrum

The spatial frequency observed at optical frequency ν is given by:

SF = νB/c

Therefore, if the visibility null at 1.22/D occurs within the passband of the instrument, the coherently integrated visibility will go through zero at that point!

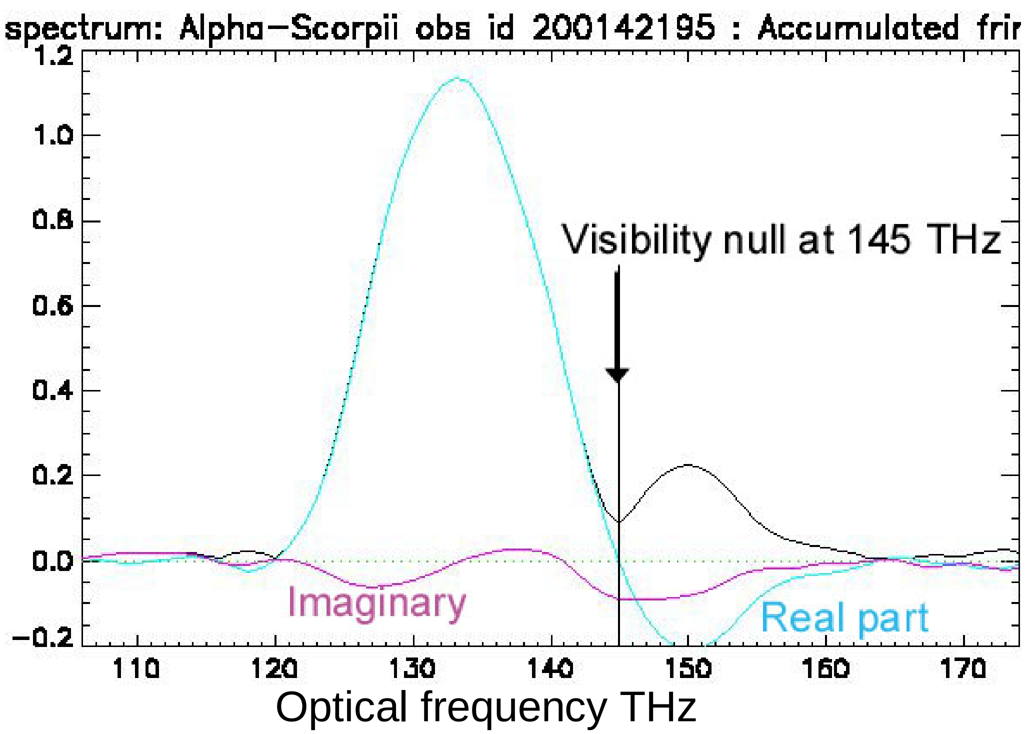

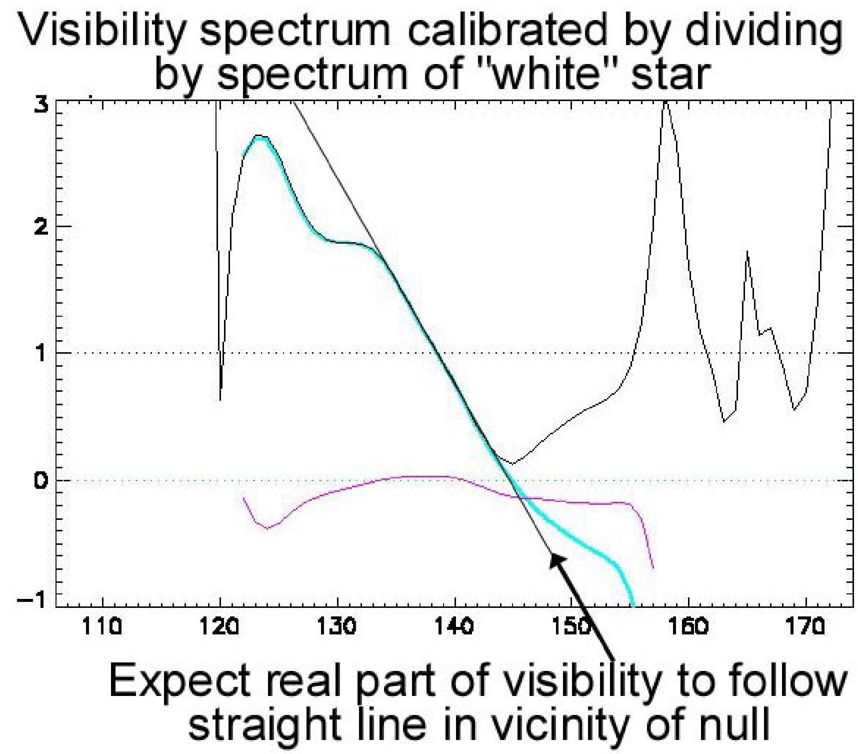

Comparison of alf sco diameters obtained from visibility nulls in spectra, with broadband visibility points

Raw visibilities (uncalibrated), alf sco, from VINCI B=16m

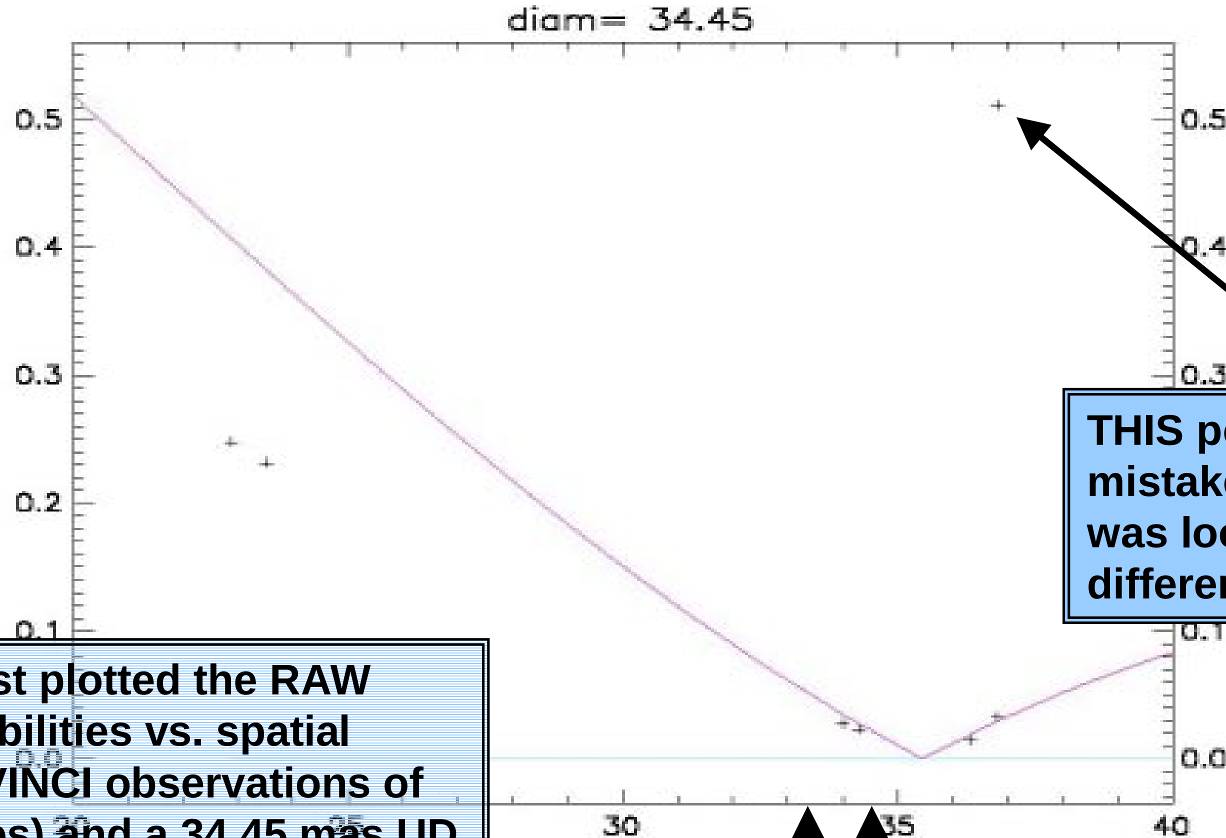

Alright, what happened here?!

THIS point was surely a mistake! Probably VINCI was looking at a different star altogether.

Here I have just plotted the RAW measured visibilities vs. spatial frequency of VINCI observations of alf sco (Antares) and a 34.45 mas UD fit, to compare with the positions of the nulls measured using the method described on the previous page.

Nulls measured in spectra

Measurement of stellar diameters by observing the null in the coherently integrated visibility spectrum

More examples:

Observations past 1st null, visibility inverted:

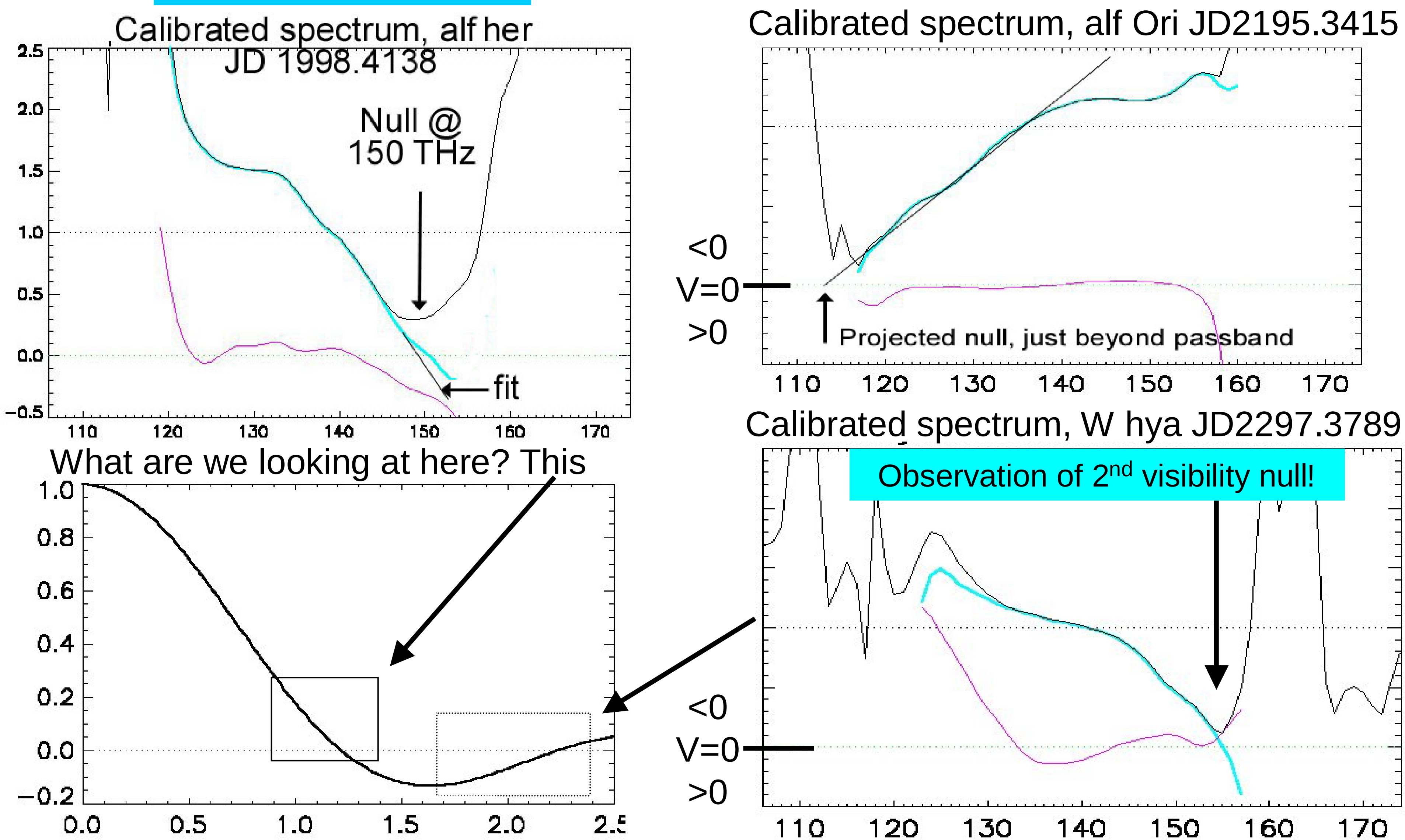

End of part I

Now we begin part 2 of my presentation. That is on the approach to calibration I am working on to obtain stellar diameters from the totallity of some 13,000 VINCI observations (visibility points) measured over the last 2 years.

First I mention some of the problems with the "standard approach" to calibrating interferometric observations. The "standard approach" says that you find a suitable "calibrator star" which is similar to your target star, but whose diameter you (think you) know for sure. From a measurement of the raw visibility of the calibrator star just before or after the target observation, you deduce the intrumental calibration or "transfer function."

1) **You generally can't find a "perfect" calibrator which matches the target star in position, color/type, magnitude, etc.**
2) **You CERTAINLY will not also find one which is the same color but is less resolved (smaller angular diameter), unless it is much dimmer!**
3) **If the calibrator is not smaller (less resolved) than the target, then the sensitivity to errors on the assumed diameter of the calibrator is >= 1.**
4) **And that is a fatal flaw, because you don't have an independent means of verifying the size of the calibrator. If you did, then you could have used that for the target as well! That would only not be true if your target had different characteristics than the calibrator, in which case 1) is violated. In other words, the chain of calibration is circular at best.**

My approach therefore is to destroy the distinction between "calibrators" and targets, and treat all stars equally with no *a priori* diameters known. Every star will be used to calibrate every other star observed on the same night. Of course some stars have more stable diameters than others (pulsating stars etc.) but we make no assumptions about the diameter of any one star.

Global calibration approach applied to VINCI visibilities

*Allowing for stellar diameter solutions which include a UD diameter, plus a **proper calibration,** which may not =1.*

Why allow for a proper calibration?

1) Many stars (not most) especially the further you go into the infrared, contain correlated flux from a compact disk, but some uncorrelated flux from circumstellar emission.

2) A specific instrument like VINCI may have a transfer function which is not flat, but somewhat wavelength dependent. Thus stars with different spectra, may show slightly different transfer functions (at the level of a few percent).

Model for instrument calibration (transfer function) and proper calibration.

Measured visibility = True visibility of star alone * net calibration

$V_{RAW} = V_{STAR} * C_{NET}$

Net calibration = Nightly calibration * proper calibration

$C_{NET} = C(t) * C_P$

Proper calibration = “type calibration” * individual calibration

$C_P = C_{TYPE} * C_{STAR}$

Type calibration is specific to a type of star due to its spectrum interacting with the instrument.

Individual calibration is due to uncorrelated flux detected photometrically but not contributing to the visibility at any baseline within a reasonable range (highly overresolved).

Measured visibility:

$V_{RAW} = C(t) * C_{TYPE} * V_{STAR} * \text{(Correlatable flux) / (Total flux)}$

Individual calibration $C_{STAR} = \text{(Correlatable flux) / (Total flux)}$ **= extrapolated visibility at zero baseline**

Detection of proper calibration.

Here is an example (which we will come back to!) of a star observed by VINCI with a very definite proper calibration

We will assume that most stars do not have a proper cal other than unity. But in the cases that we do detect one, this will affect our determination of the star's true diameter!

Note that MIDI will have to deal with this much more than instruments operating at shorter wavelengths!

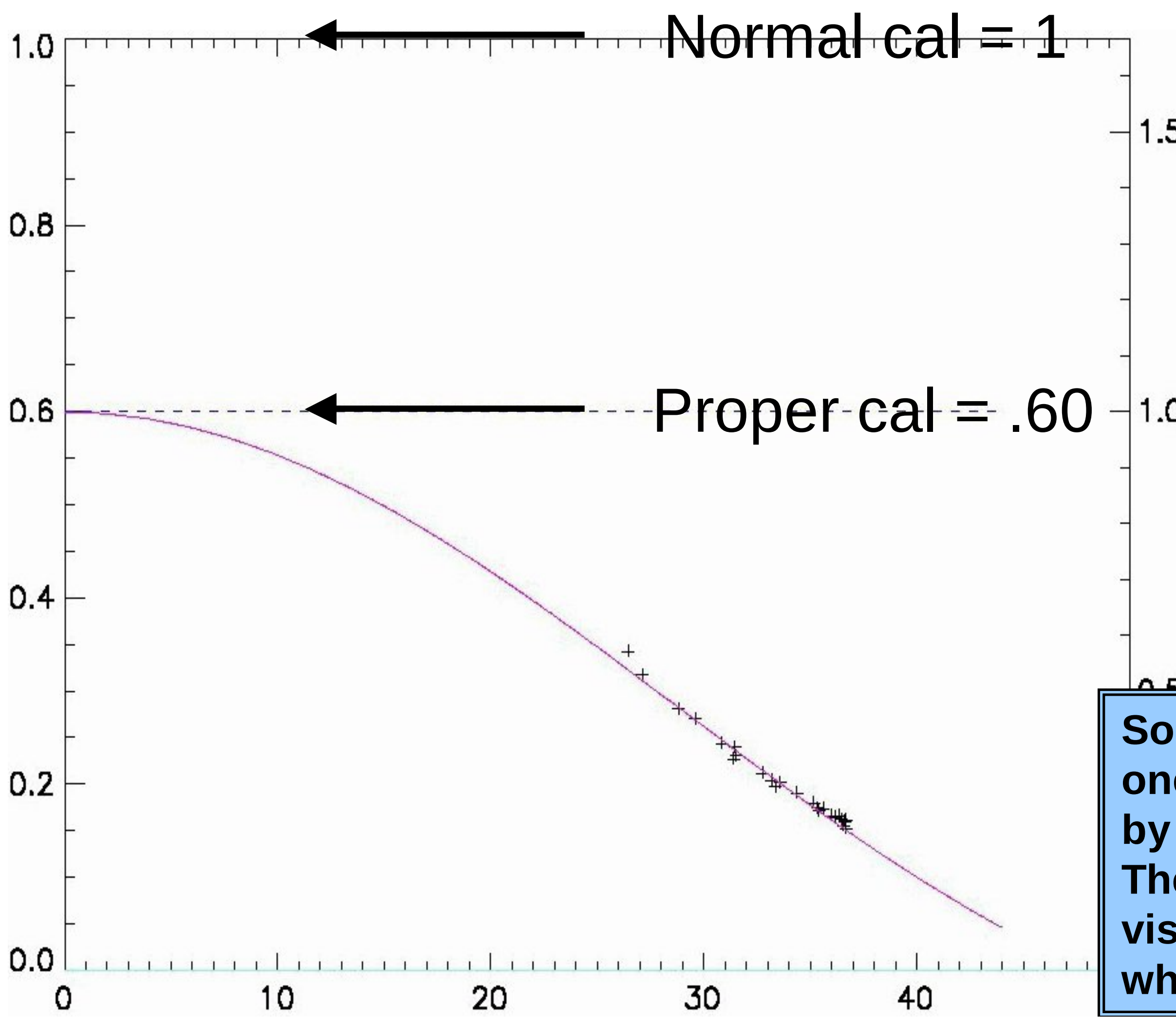

So here are visibility points from one particular star AFTER dividing by the "normal" nightly calibration. They do not lie on a "normal" visibility curve, but rather one which is also multiplied by .60.

What is plotted on the next page, are the contours of the likelihood function for the joint solution of net calibration (vertical) and stellar UD diameter (horizontal). With only one visibilty point (or visibility points near a single spatial frequency) as in the upper left, we have a remaining degree of freedom given by the crescent, from a lower calibration with a small diameter, up to a calibration of 1.0 with a large diameter. The true solution must be somewhere in between. By including more measured visibilities at a range of spatial frequencies, (upper right) the solution is narrowed down somewhat, but still supplies no good estimate of the diameter. With further spatial frequency coverage (lower left) a better estimate of the diameter (and calibration) emerges.

Finally with a superior data set (lower right), we can simultaneously solve for the diameter and net calibration with a reasonable error level. Even in this case, there is some remaining uncertainty in one direction (lower left to upper right). Thus an additional independent measure of the calibration for that night (i.e. from other stars also observed) which is also applicable to this star, can be used to constrain the vertical position of the solution on this locus, and force a finer determination of the stellar diameter.

The contours that are plotted are for the 1 and 2 sigma boundaries of the likelihood function.

We can solve for the likelihood of a joint diameter – calibration solution from a set of observations spanning some range of baselines. If we can be sure that the star does not have a proper cal outside of 1, this supplies the transfer function for that night…

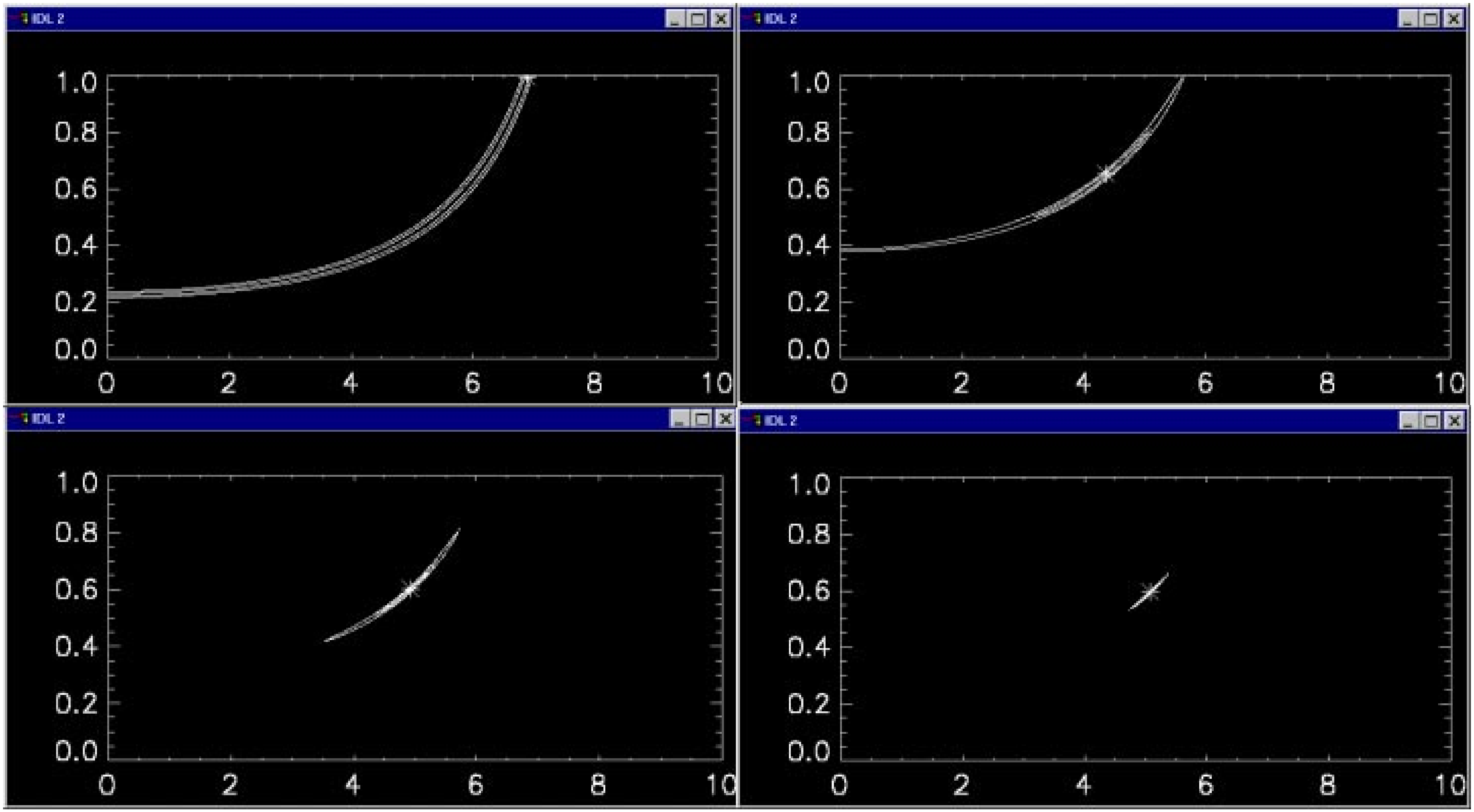

Global calibration approach applied to VINCI visibilities obtained through quasi-coherent integration.

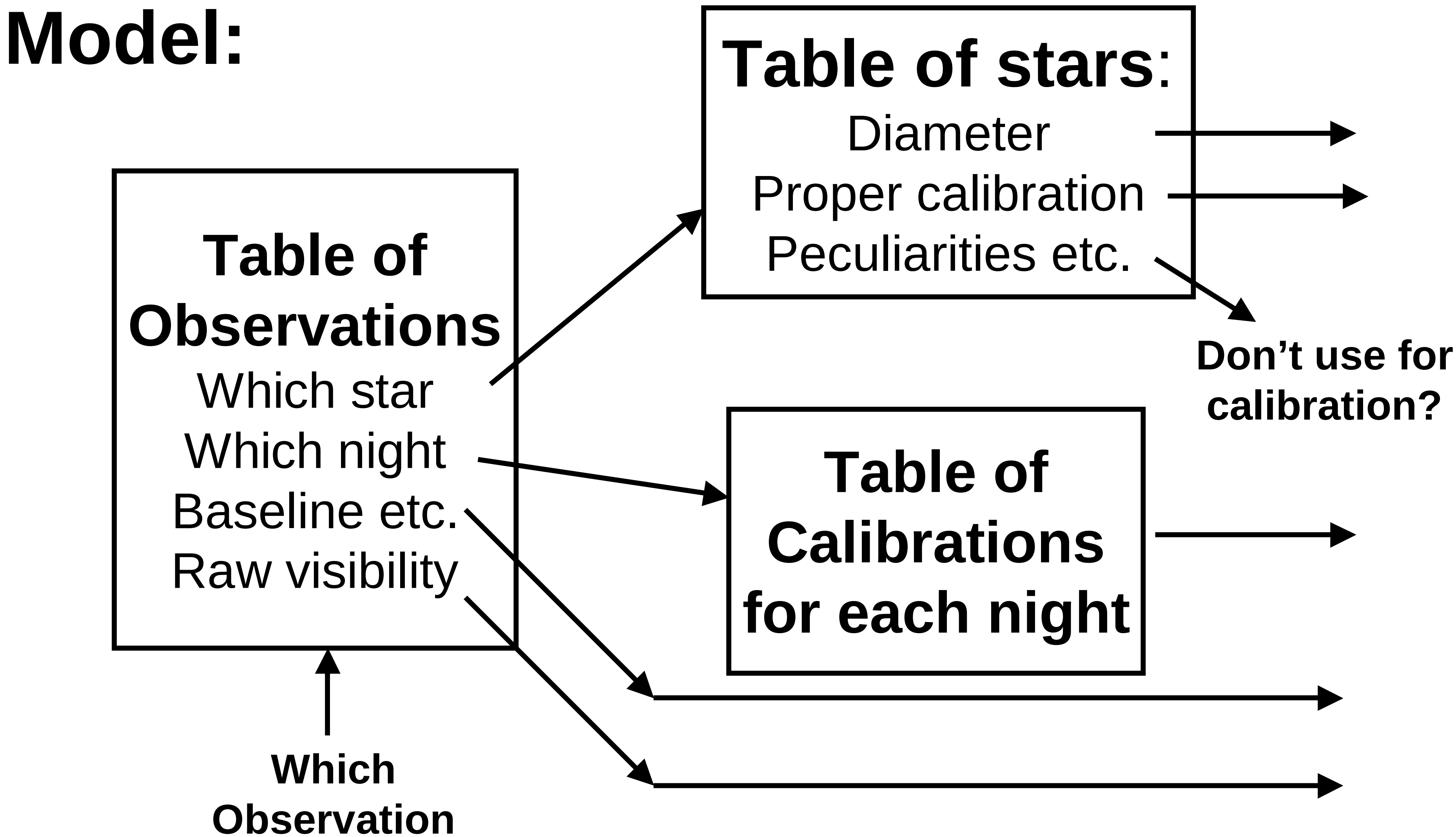

Model (continued)

Table of stars:
Diameter
Proper calibration
Peculiarities etc.

Diameter D_{star}

Proper cal C_{star}

Don't use for calibration?

Table of Calibrations for each night

Nightly cal C_{nite}

Baseline $|B|$

Measured vis V_{raw}

Resolvability $R = D/(\lambda/B)$

Residual $= V_{raw} - (2J_1(\pi R)/\pi R)\, C_{nite}\, C_{star}$

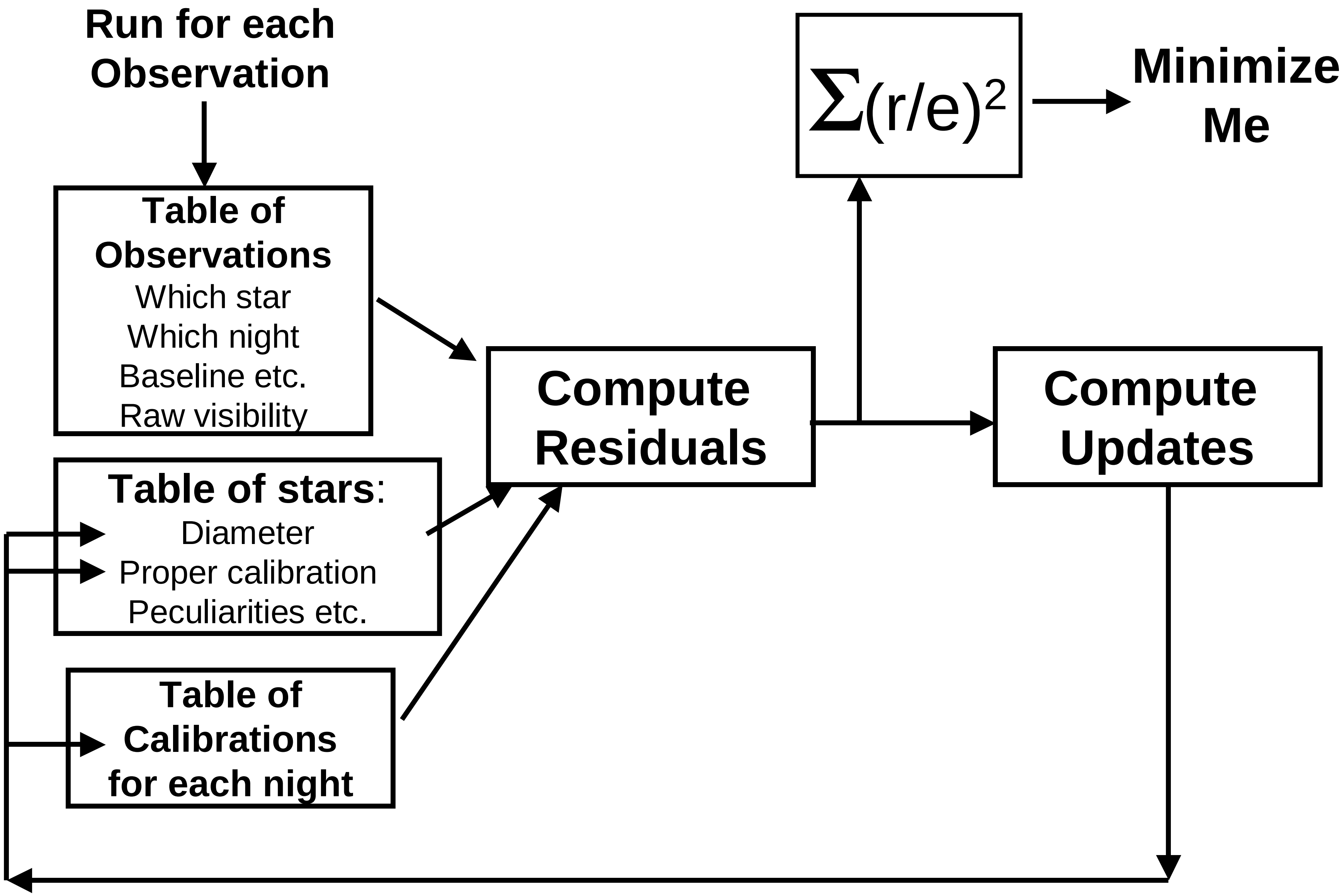

Global calibration and diameter solution: Method

In the previous slides we have seen the model which is applied and method for globally solving for nightly calibrations, stellar diameters for each target observed, and (in some cases) proper calibrations for those stars which are distinct from unity.

Presently I am in a very early stage of performing this computation. My current algorithm (which has lots of room for improvement!) however does approach a solution after 30-40 iterations. This is illustrated by the graphs on the next page, which show the algorithm converging toward the diameter of several stars over the course of 40 iterations. The diameter estimate (assuming no proper calibration) are given by the magenta plots. The white plots and squares, where shown, are solutions for the diameter in conjunction with a non-unity proper calibration (not shown) which may or may not be real.

On the following page, is a plot of the transfer function (nightly calibration) determined also as part of this computation, as a function of time (Julian day - 2450000) for two periods in the operation of VINCI. This reflects hardware changes in the beam combiner (and other optics) plus noise. Wide horizontal sections are simply due to no data having been taken over that period and the adoption of the calibration for the nearest night on which a solution was obtained. Vertical blue lines delineate the positions of known hardware adjustments which are *expected* to alter the transfer function (obviously not all such hardware adjustments were known by this database!).

Convergence of diameter solutions over many iterations

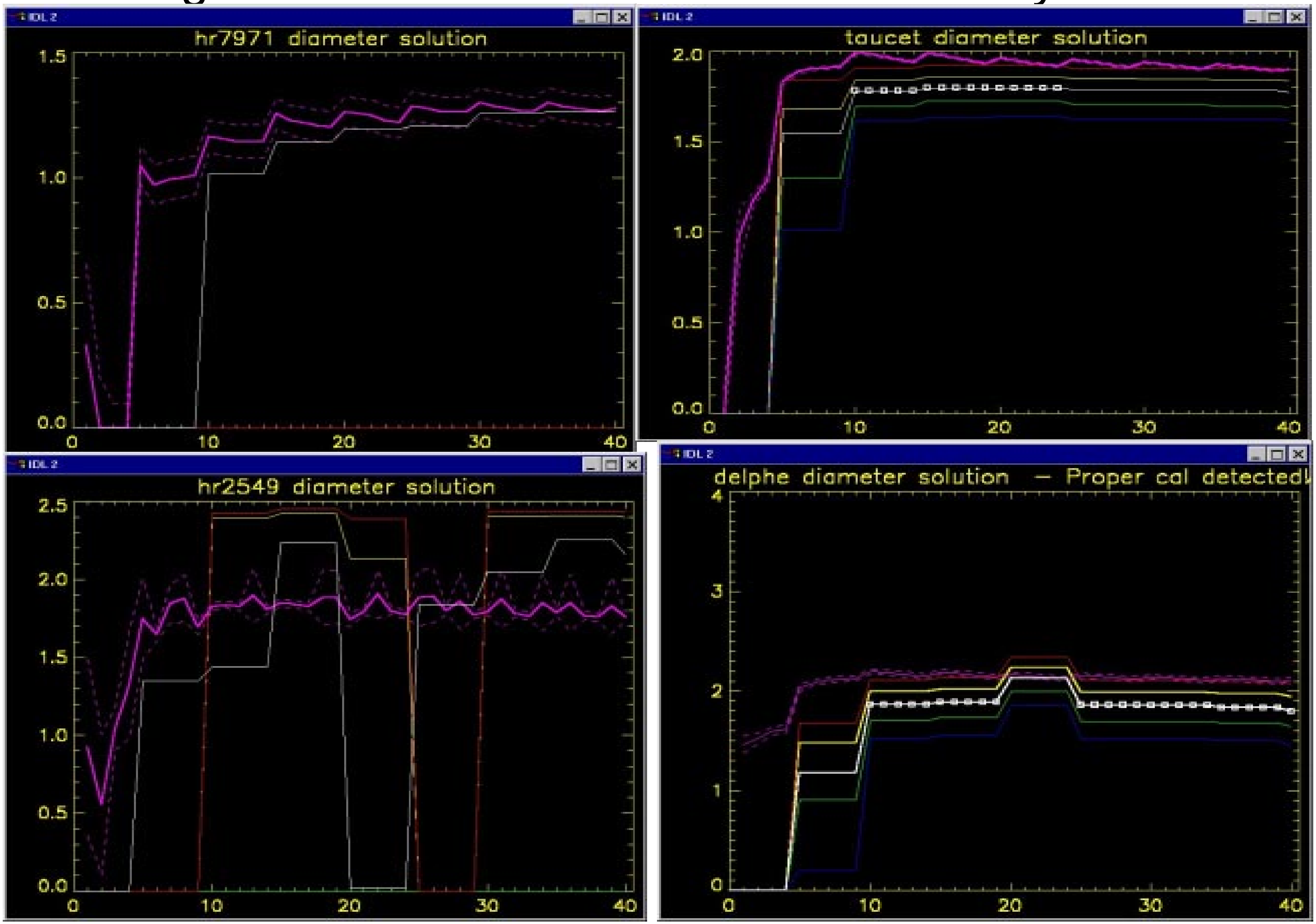

Results from VINCI using global cross-calibration algorithm (in its very early stages!)

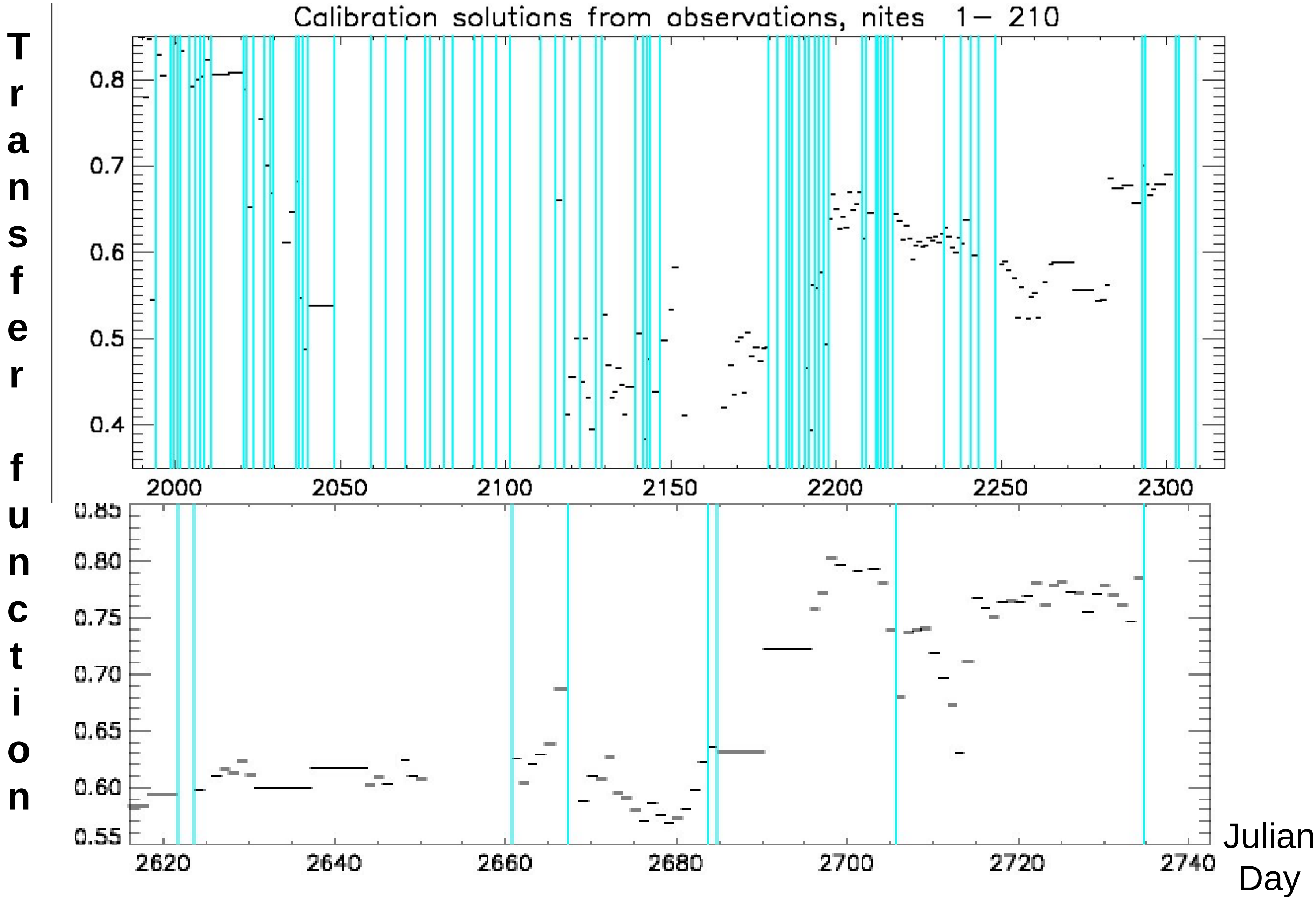

Early (unofficial!) results from global calibration solution on 8, 16, and 24 meter baseline data. Only diameters > 9 mas shown.

Results marked with an 'X' in pink are known to be mistaken for various reasons which the current algorithm cannot handle. All of the rms error bars shown are overly optimistic due to a limitation in the code. Please wait for the official results to be released in the not-distant future after further progress in the algorithm and better identification of bad input data points. ☺

gameri 9.18 +/- .07 mas
119tau 9.68 +/- .06 mas
rpeg 9.79 +/- .19 mas
chiphe 9.84 +/- 2.06 mas
akhya 9.91 +/- .15 mas
lamaqr 9.95 +/- .45 mas
62sgr 10.14 +/- .13 mas
alfhya 10.15 +/- .14 mas
tcet 10.28 +/- .18 mas
v744cen 10.29 +/- .41 mas
X delvir 10.47 +/- .81 mas
19psc 10.51 +/- .20 mas
sori 11.05 +/- 0. Mas
X deloph 11.06 +/- .11 mas
-- Proper cal = 1.144 with D = 14.4 mas
tlep 11.08 +/- .06 mas
wori 11.08 +/- .16 mas
siglib 11.40 +/- .14 mas
etagem 11.91 +/- .42 mas
etasgr 12.27 +/- .40 mas
rscl 12.62 +/- .14 mas
-- Proper cal = .947 with D = 11.1 mas
2cen 13.53 +/- .16 mas
rxlep 13.56 +/- .07 mas
X del2gru 13.59 +/- 2.16 mas
rcnc 13.86 +/- .09 mas
alfcet 14.24 +/- 1.24 mas
13gem 14.29 +/- .11 mas
nu.pav 14.58 +/- .17 mas

uori 16.70 +/- .29 mas
X raqr 18.62 +/- .11 mas
-- Proper cal = .964 with D = 17.9 mas
rlep 18.97 +/- .19 mas
-- Proper cal = .761 with D = 13.8 mas
vhya 19.05 +/- .07 mas
X lamvel 20.01 +/- 1.90 mas
alftau 20.33 +/- .05 mas
gamcrua 24.68 +/- .12 mas
rleo 25.77 +/- .24 mas
betgru 25.80 +/- .04 mas
-- Proper cal = .924 with D = 25.2 mas
X rhya 26.93 +/- .01 mas
X l2pup 27.47 +/- .22 mas
X alfcar 27.54 +/- .10 mas
X omicet 29.49 +/- .25 mas
-- Proper cal = .501 with D = 24.8 mas
alfsco 34.52 +/- 0. Mas
X alfori 42.31 +/- 1.37 mas
-- Proper cal = .669 with D = 30.6 mas

On the next page, we look at the likelihood contours (1, 2, and 3-sigma countours are drawn) for two stars with a definite non-unity proper calibration.

On the following page, is an example of a very stable and well observed star (used as a “calibrator) tet cen, with 575 observations on the 66 meter baseline. Almost all of those datapoints lie right on the theoretical visibility curve (purple) for a 5.16 mas UD object, with the positions of the outliers being conspicuous (and clearly non-gaussian distributed!). A plot of “apparent diameter” versus Julian date (used to identify pulsating diameters) shows a steady curve (except for a few days where bad datapoints dominated the solution).

The 2 following pages likewise have plots for a star’s apparent diameter versus date which are NOT constant but shows a consistent change over time. The visibility points, taken together, do NOT lie on a single curve (different symbols correspond to observations on different nights).

Miscellaneous results found in global solutions

Detected proper cals from various stars…

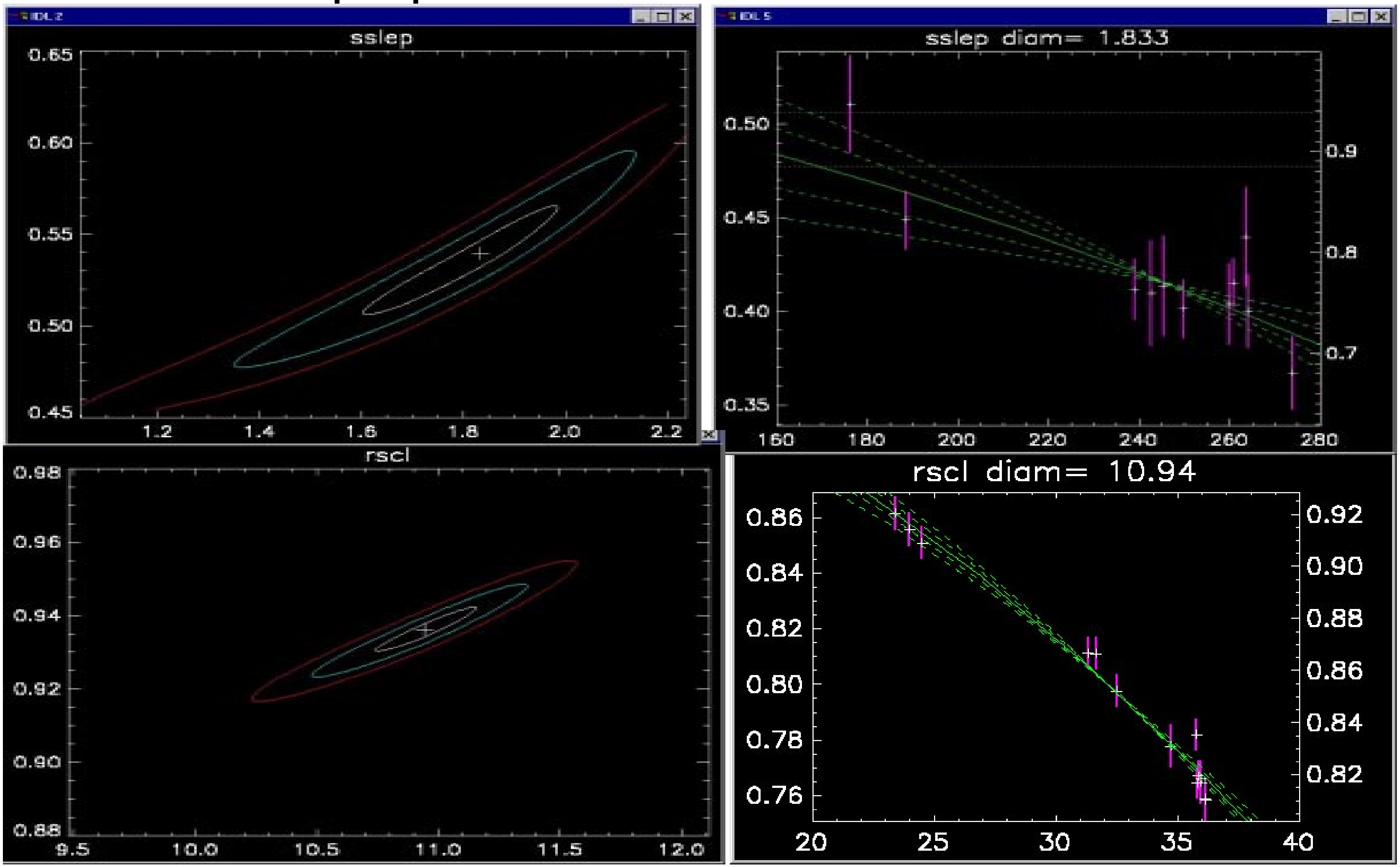

Miscellaneous results found in global solutions

Good fit from a well-behaved star that was observed many times (considered a “calibrator”)

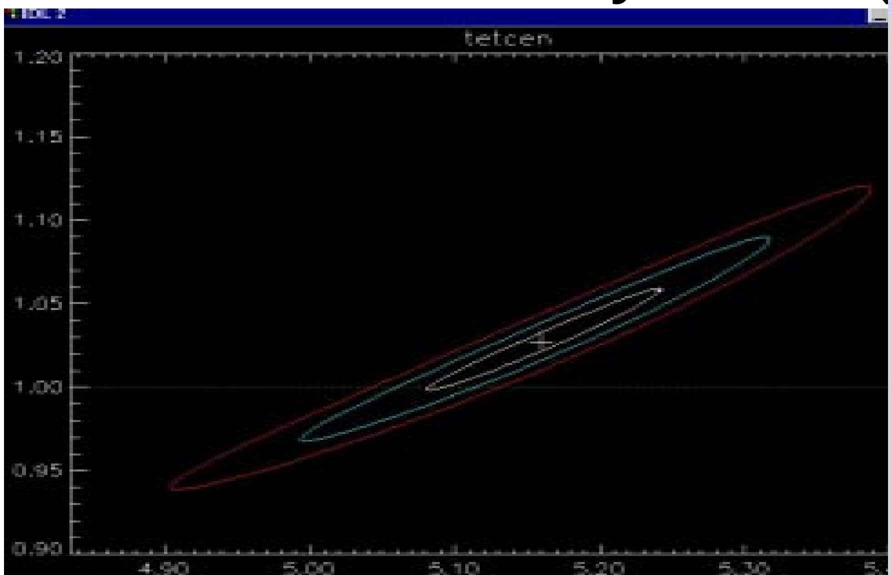

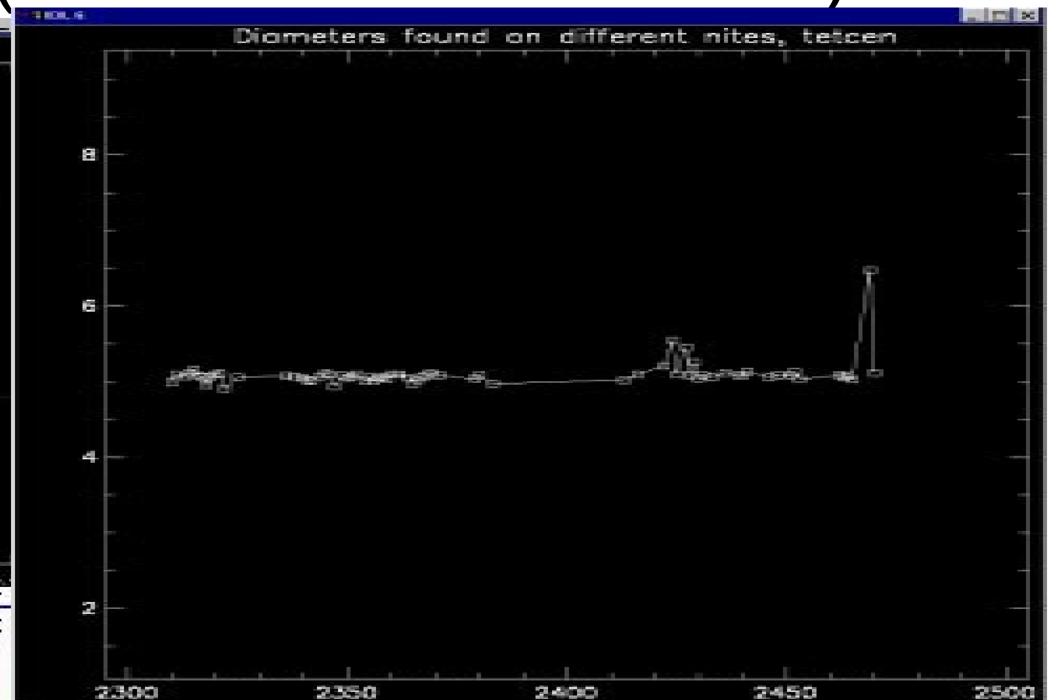

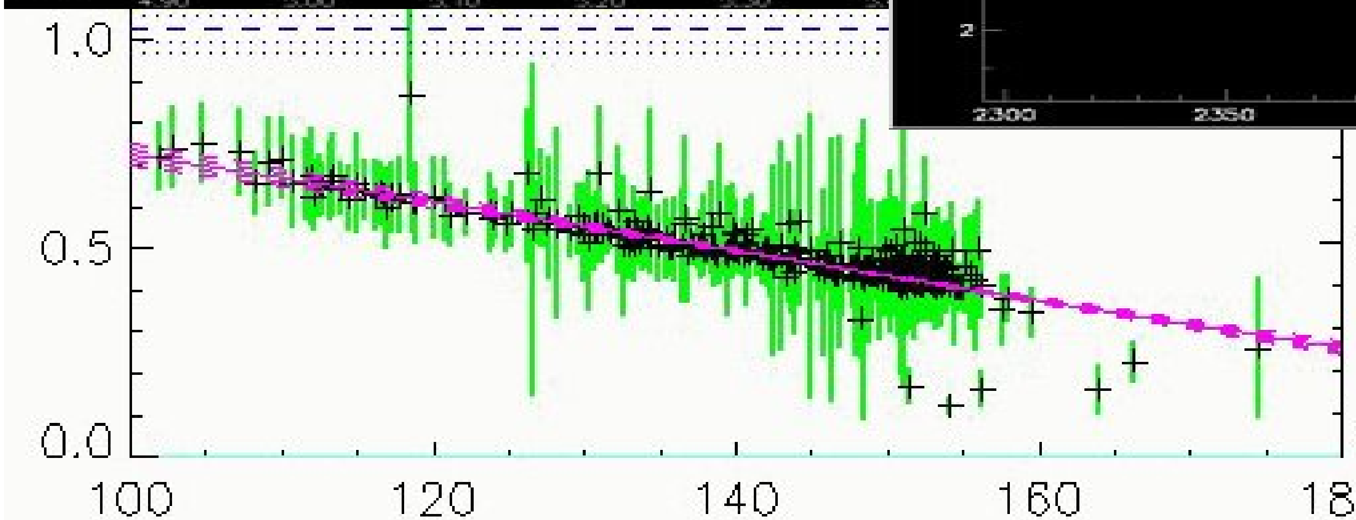

These are all from tet cen on the 66 meter baseline..

Miscellaneous results found in global solutions

This star's diameter is doing something funny….

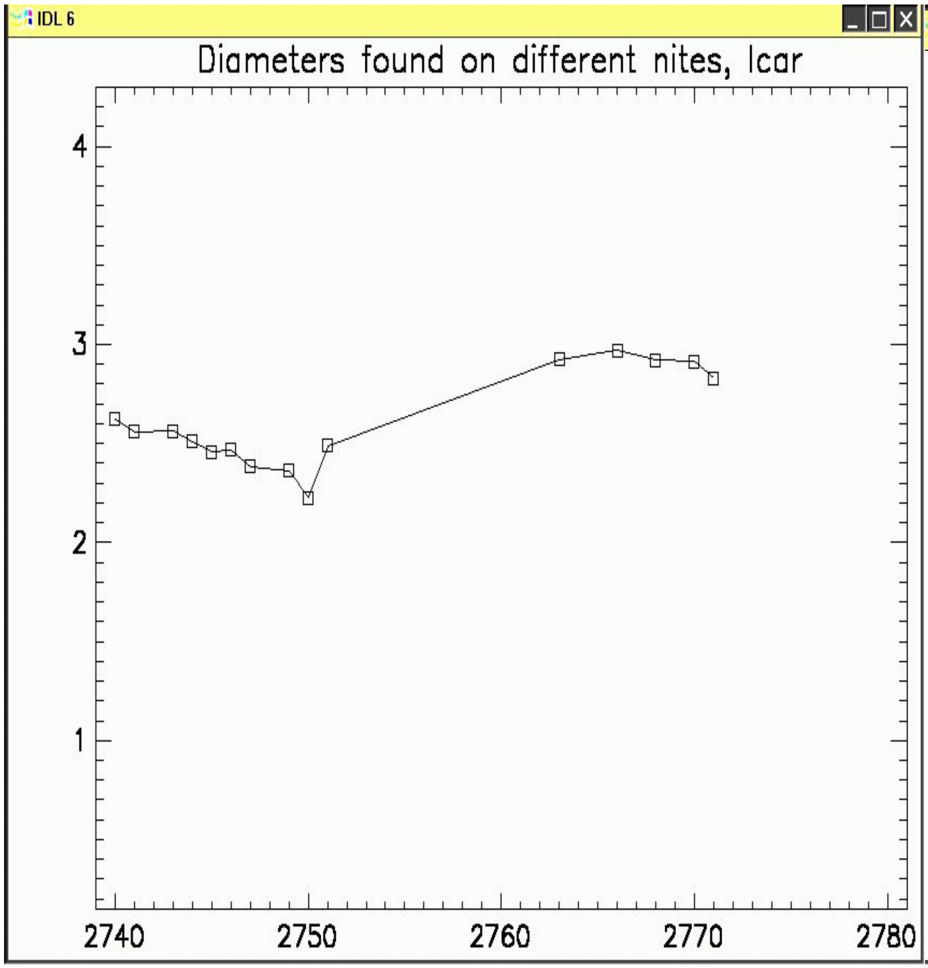

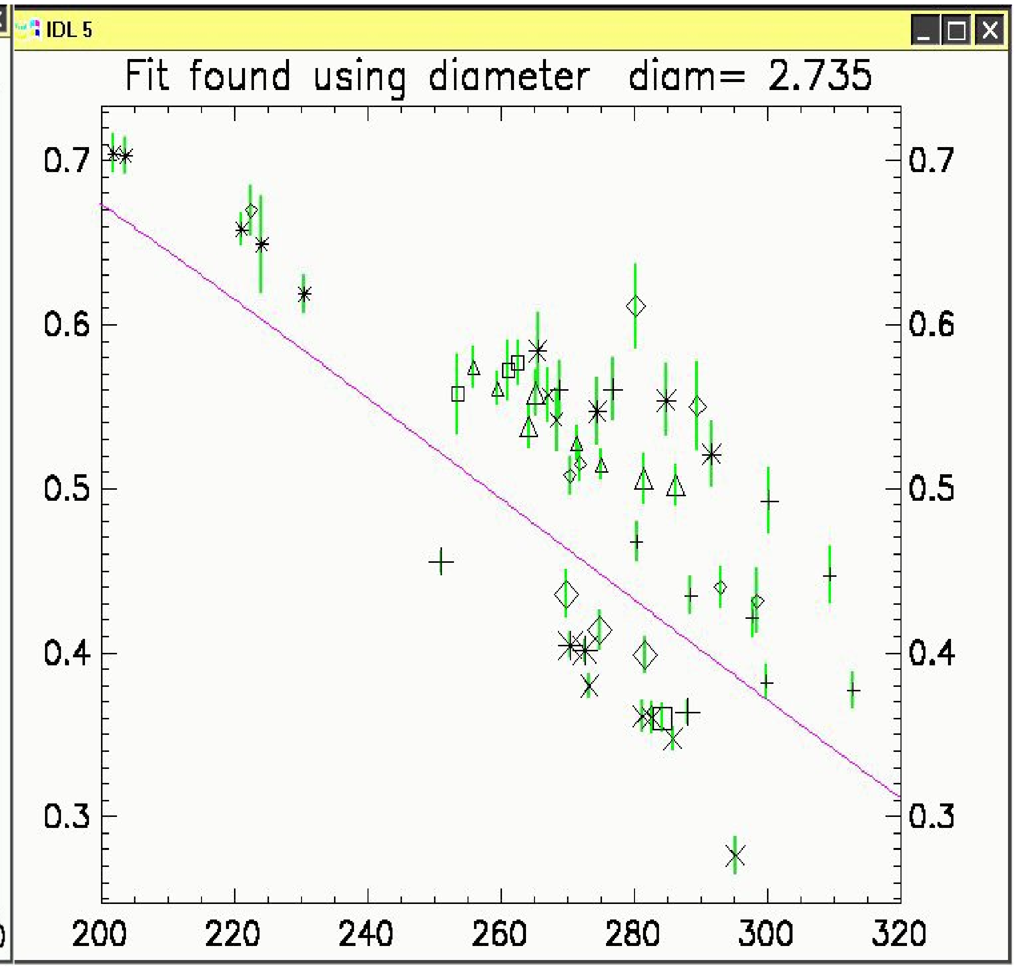

(It's a cephied)

Miscellaneous results found in global solutions

Another funny diameter… L2 pup

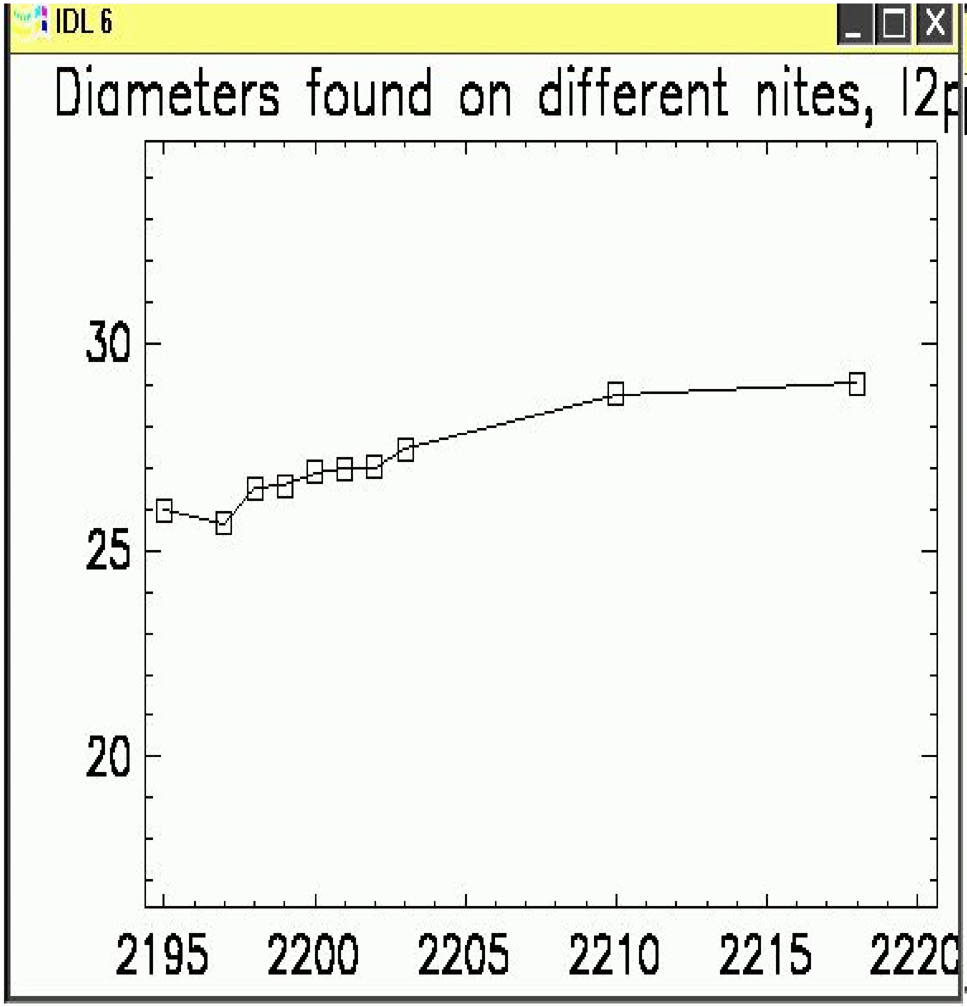

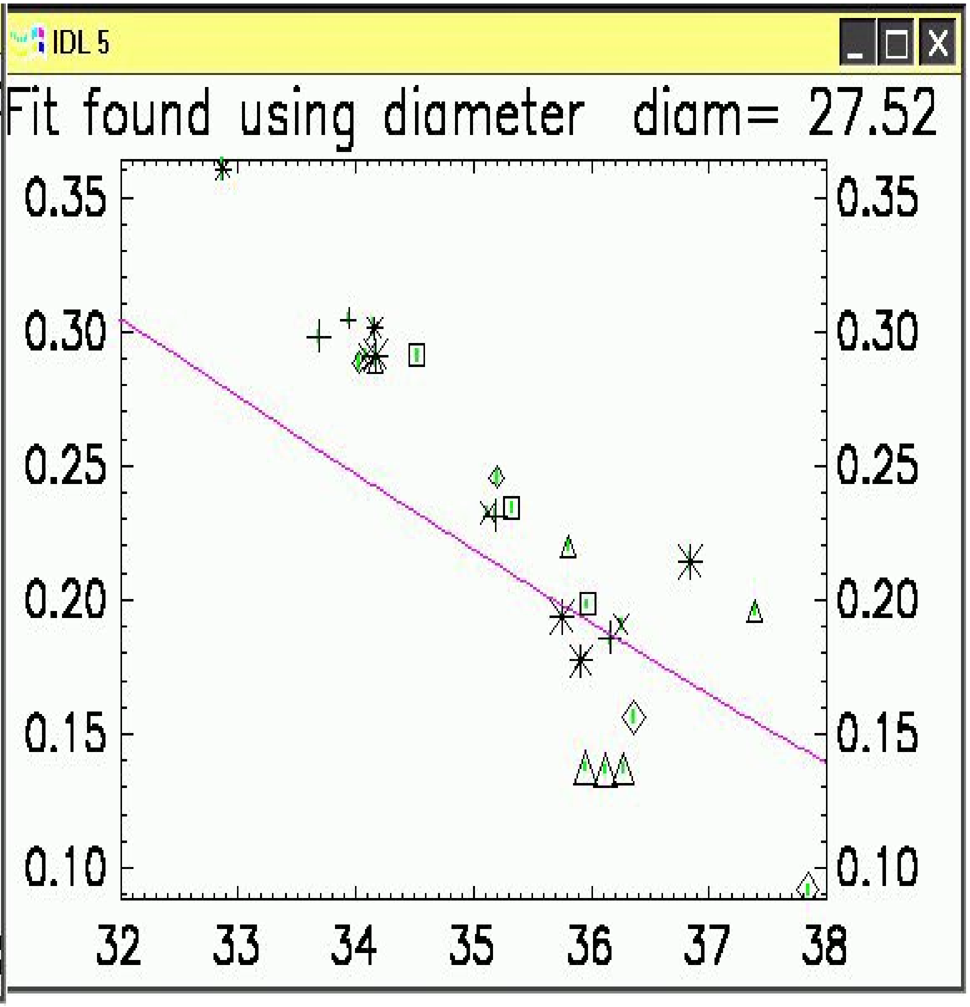

Miscellaneous results found in global solutions

A visibility fit that doesn't ... alf eri (Achernar)

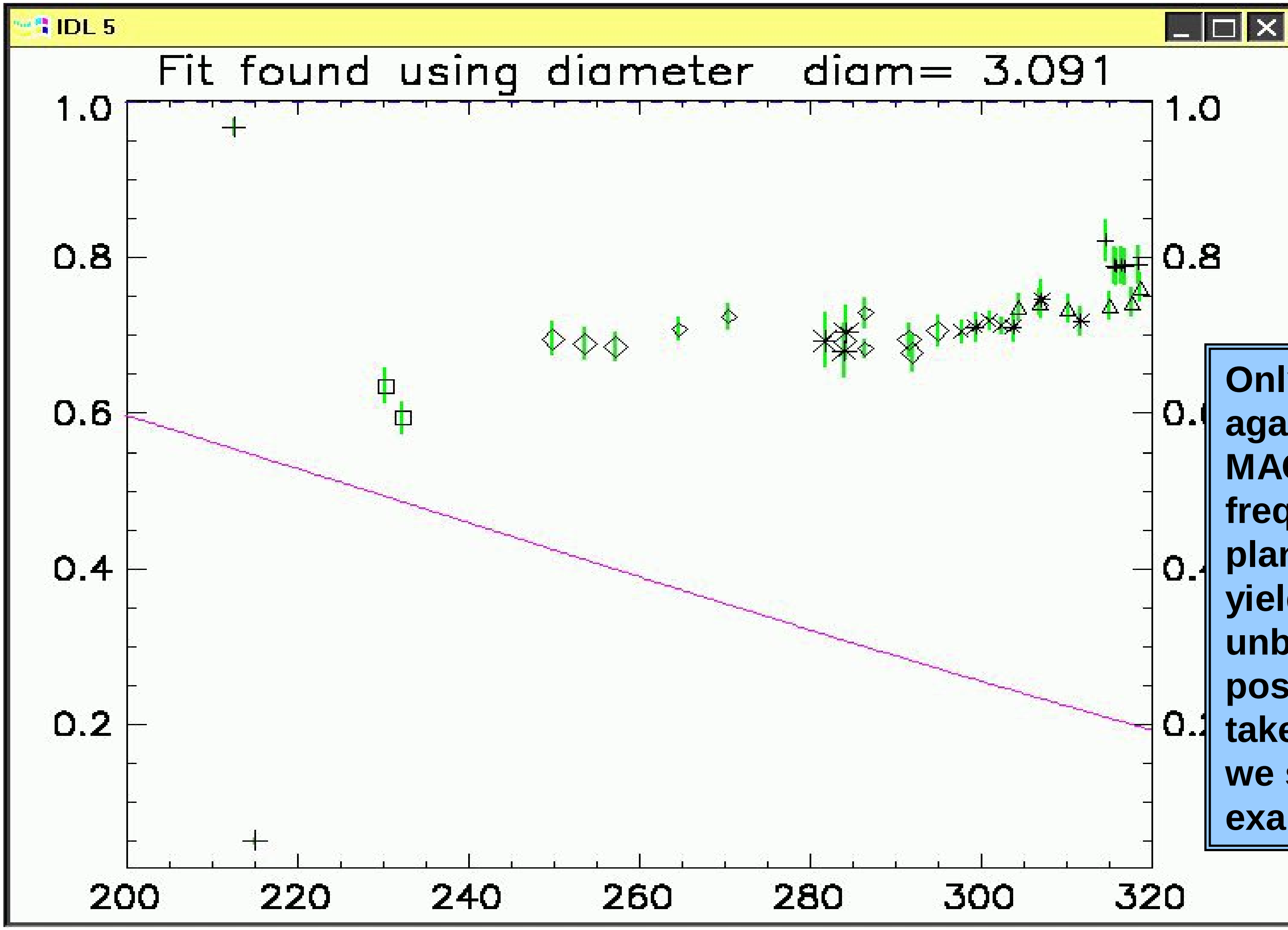

Only plotting visibility against the MAGNITUDE of spatial frequency in the UV plane, may sometimes yield surprising (= unbelievable) results if position angle is not taken into account, as we see in this example….

Miscellaneous results found in global solutions

Alf eri ….. on closer examination:

On the 140 meter baseline: **On the 66 meter baseline:**

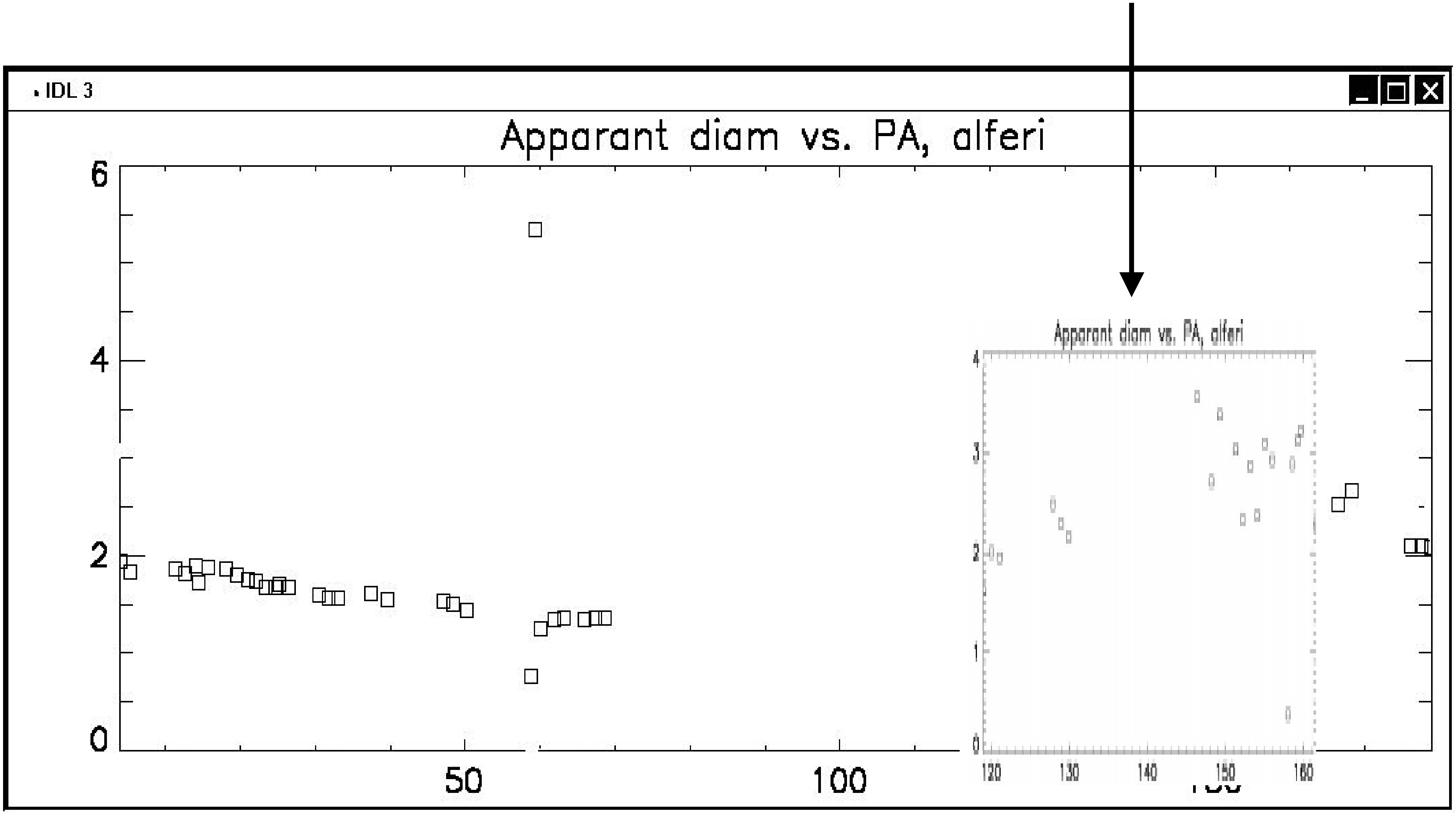

As we can see, alf eri has a strong position angle dependence on diameter. My preliminary diameters versus position angle (0 to 180 degrees) are plotted on the previous page. In discussion during the conference, a mistake in interpretation found in a recently published paper was noted. The apparent UD diameter measured from interferometry of an ellipse at various position angles should be of the form:

$$D(\phi) = D_0 + a \sin(2(\phi - \phi_0))$$

Where the major and minor axes of the ellipse are $D_0 + a$ and $D_0 - a$. However when such radii are plotted in polar coordinates vs. position angle ϕ, you do NOT get the figure of an ellipse (as the published paper attempted to fit) but rather a *reciprocal conjugate ellipse* which only matches the ellipse at $\phi = \phi_0$ and at $\phi = \phi_0 + 90^0$. The difference between these two figures is shown on the following page.

One can imagine a sine wave of 1 complete cycle superimposed on the graph of the previous page to fit the measured data points. With refined diameters obtained from running an improved version of the global calibration algorithm, we hope/expect to obtain just such a determination of the elliptical shape of this rapidly rotating star.

Comparison of elliptical shape of star, and reciprocal elliptical shape of the diameter detected with a baseline at the corresponding position angle (dotted).

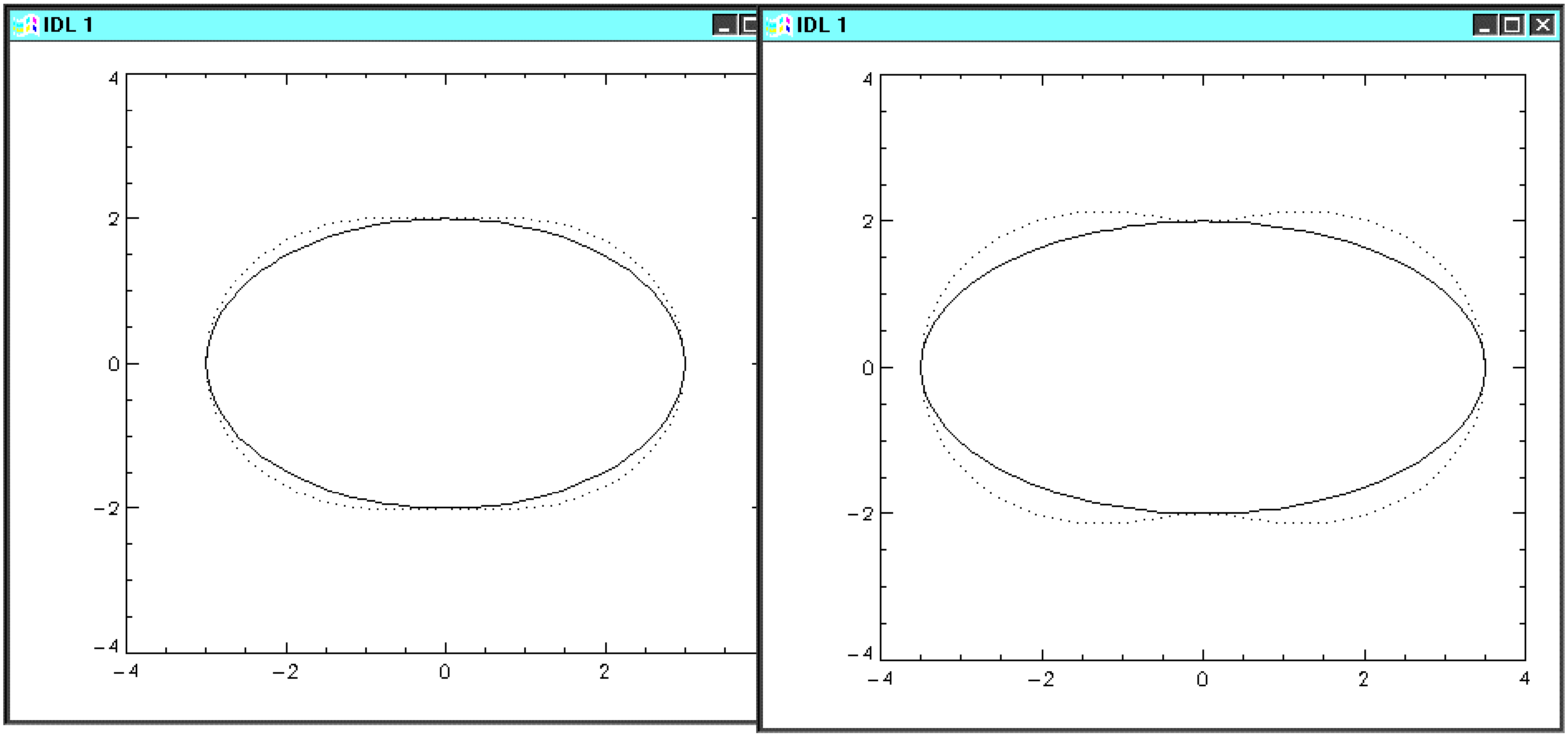

To get good estimates of stellar diameters, we need:

1) Good baseline coverage on the object (not just a long baseline) in order to ascertain its proper calibration. Also different physical baselines in order to rule out (/in) position angle dependencies.
2) High accuracy of visibility points (on both the object of interest and other "calibrator" observations). **Note**: All interferometers with good visibility accuracy (1% or better) have employed spatial filtering.

Baseline diversity 1

Many measurements taken at approximately the same projected baseline may be good for beating down the diameter errors due to measurement noise. But they are useless for estimating the proper calibration or verifying a model in general! The sensitivity of a set of observations to proper calibration is proportional to $R^2_{max} – R^2_{min}$ where R is the resolvability defined as $D/(\lambda/B)$ where D is the diameter of a star.

Therefore, unless we are able to rule out a proper calibration *a priori*, it is wise to observe a source at widely separated points on a single night, not just the “best time” when it is high in the sky.

Baseline diversity 2

Even many measurements taken with the aid of earth-rotation synthesis on a single **physical** baseline, will have trouble differentiating between a true diameter-calibration solution, and other source structure which may mimic a simple diameter-calibration solution.

For instance, this “solution” for eta car with a “detected” proper calibration of .52, matched the VINCI data on the 8 and 24 meter baselines. But it would predict a very low visibility on the 66 meter baseline where a visibility close to .2 was measured!

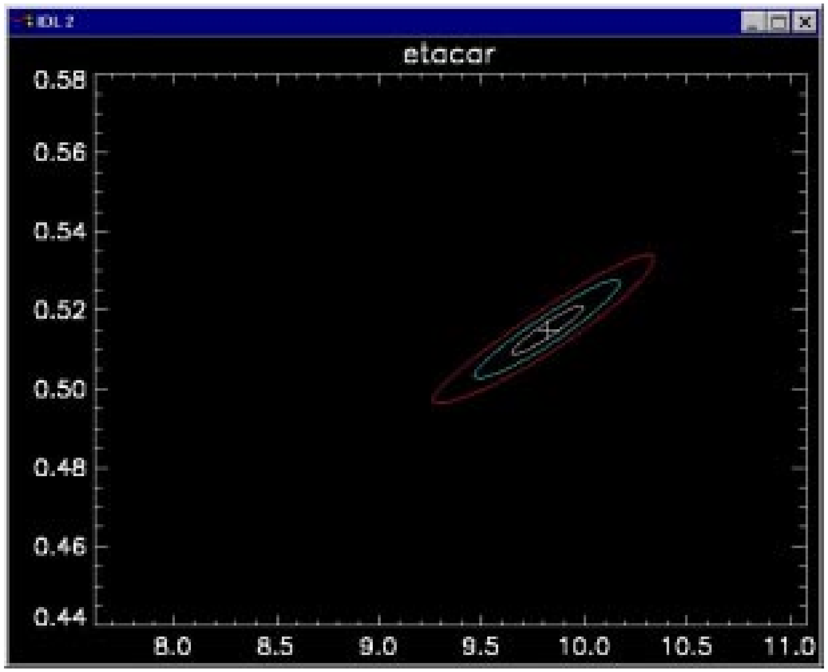

Illustration of importance of accuracy of visibility points.

Actual VINCI visibilities on Mira (omi ceti), JD2205 – 2206
(Degraded version)

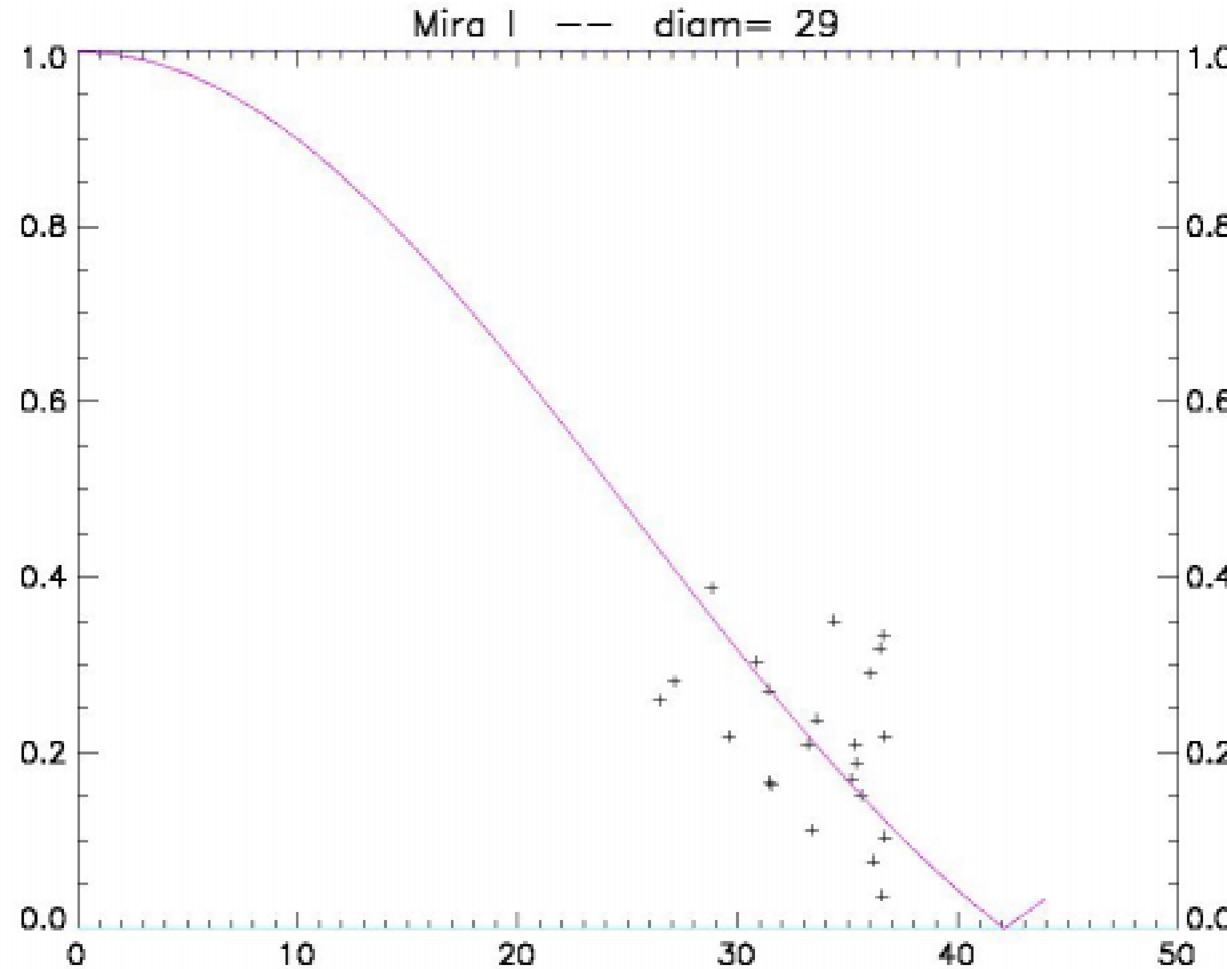

On the following few pages, is an illustration regarding what can be obtained (or lost!) depending on the accuracy of visibilities measured with an interferometer. Here I have taken REAL data points from VINCI on the star omi ceti (Mira). But with the help of a random number generator, I have added noise to the data as if it had been obtained from an instrument whose accuracy was MUCH poorer. The visibility curve you see superimposed on the data, corresponding to a 29 mas UD, appears as a "reasonable" fit. But ….

Illustration of usefulness of accuracy of visibility points.

Actual VINCI visibilities on Mira (omi ceti), JD2205 – 2206
(Better version – less noise)

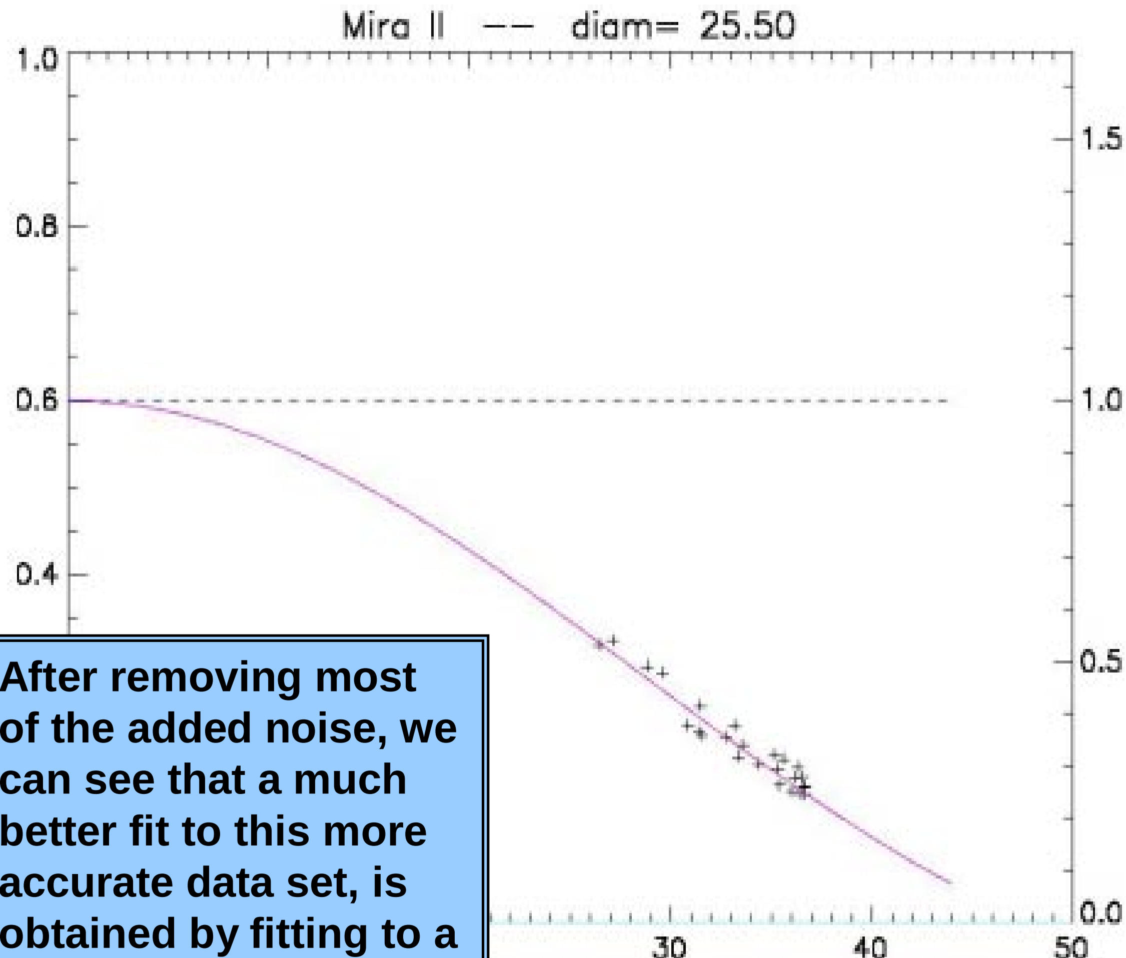

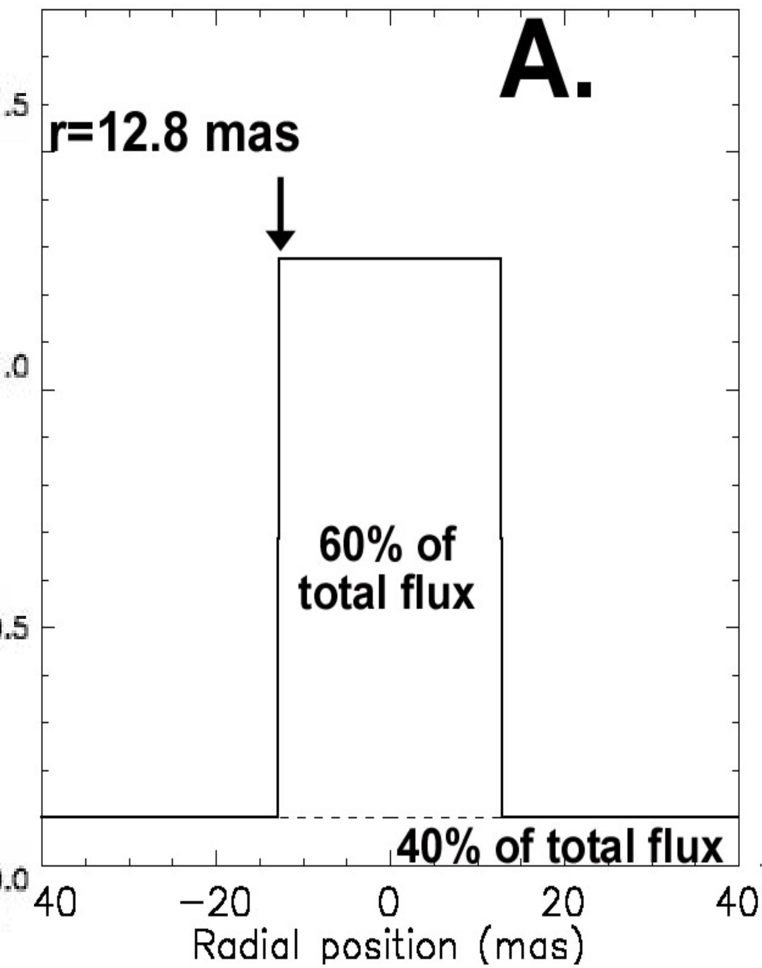

After removing most of the added noise, we can see that a much better fit to this more accurate data set, is obtained by fitting to a proper calibration of .60 and a diameter of 25.5 mas. But …..

Proper calibration = .60

Illustration of usefulness of accuracy of visibility points.

Actual VINCI visibilities on Mira (omi ceti), JD2205 – 2206
(Best version: actual visibilities obtained! No noise added)

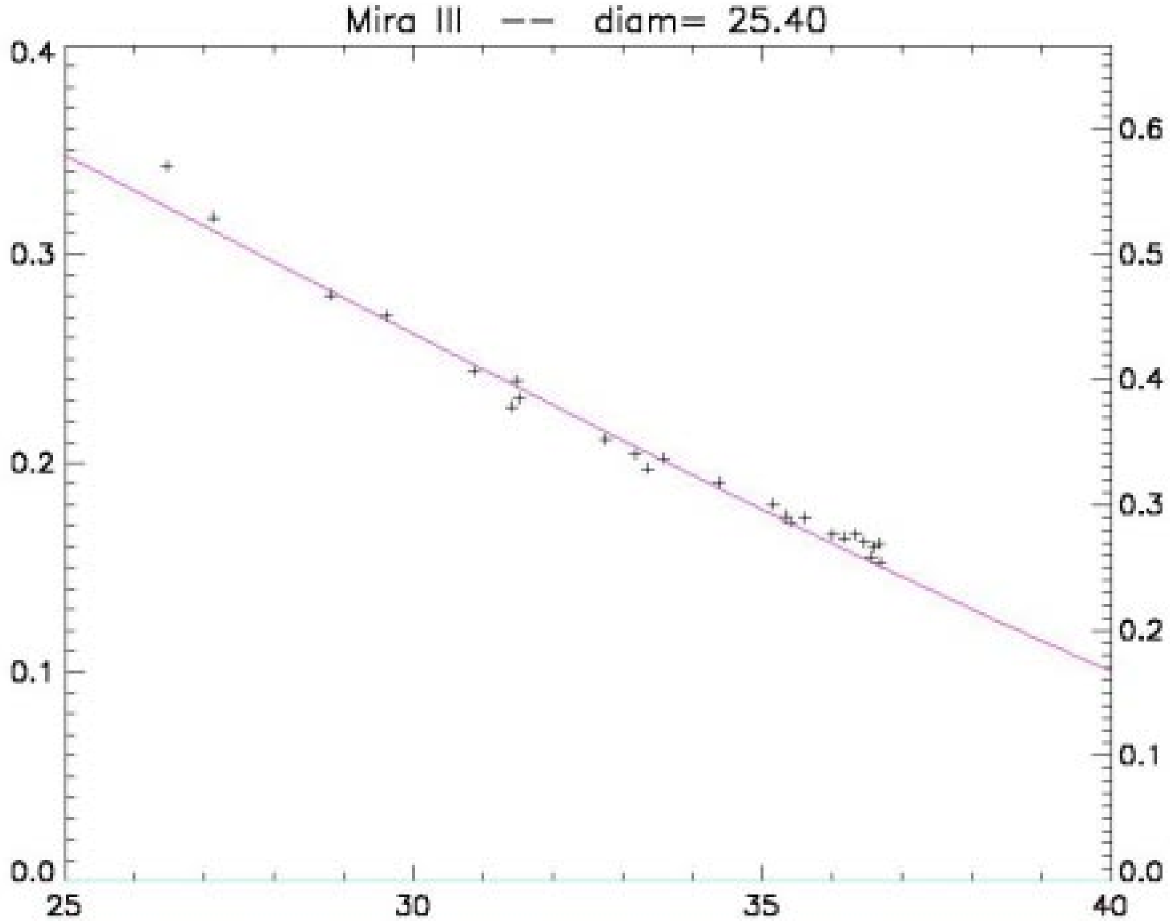

Now this is fit with a 25.4 mas UD model with a proper calibration of .60. The fit is not bad. But….

Though this fit is not bad, now looking at the data points with NO added noise, we can detect a more subtle departure from the model. The residuals we now see are NOT white noise …

Illustration of usefulness of accuracy of visibility points.

Actual VINCI visibilities on Mira (omi ceti), JD2205 – 2206
(Best version: actual visibilities obtained! No noise added)

… which permits us to invoke a 3-parameter solution, in which we add a uniform disk plus a gaussian disk. Such a solution could not have been solved for using data points of much poorer accuracy!

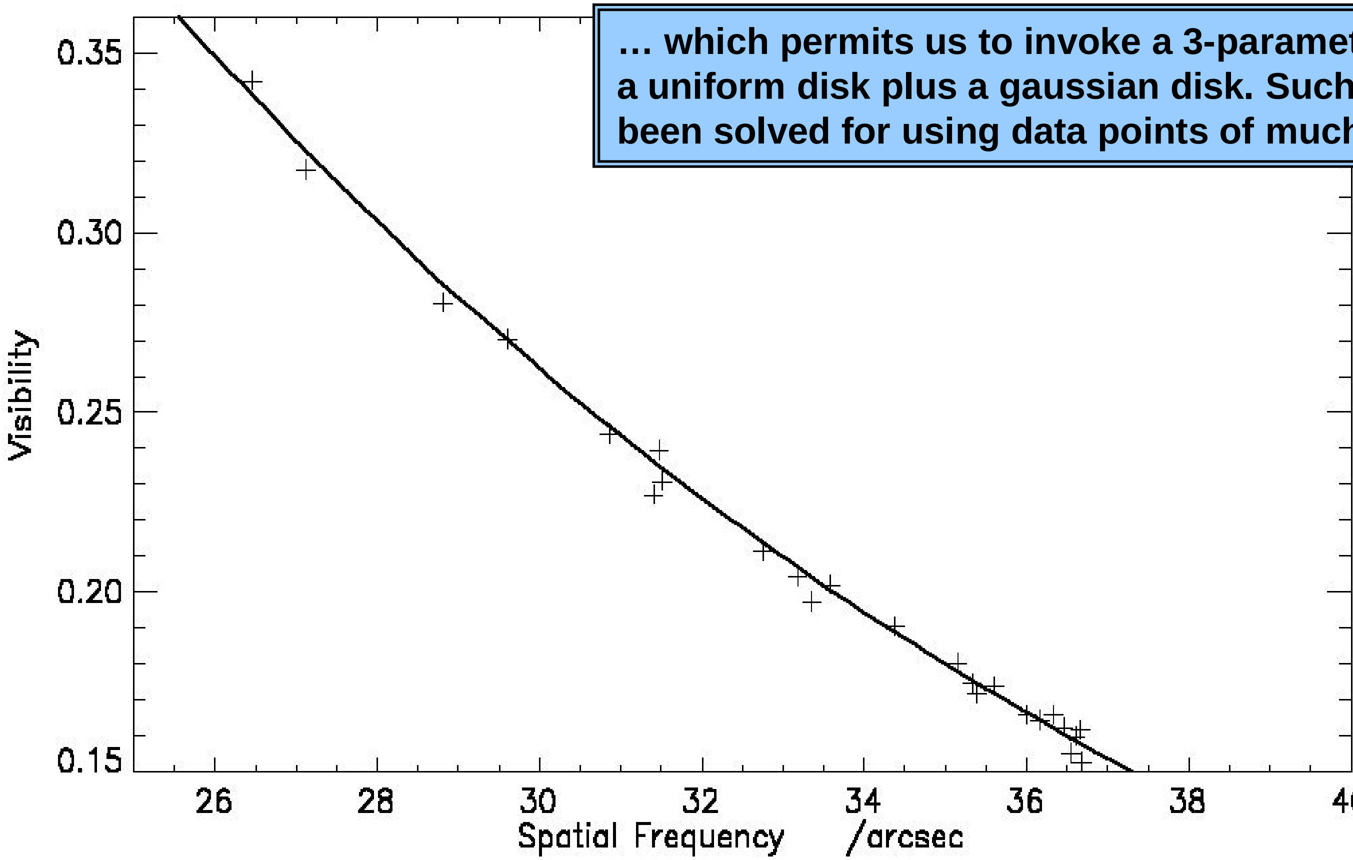

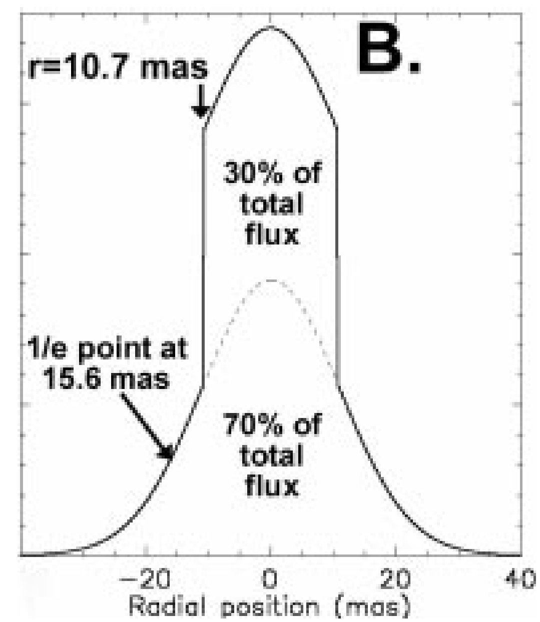

Now we have reduced the residuals by a factor of 2, by going from a 2-parameter model to a 3-parameter model (as shown)

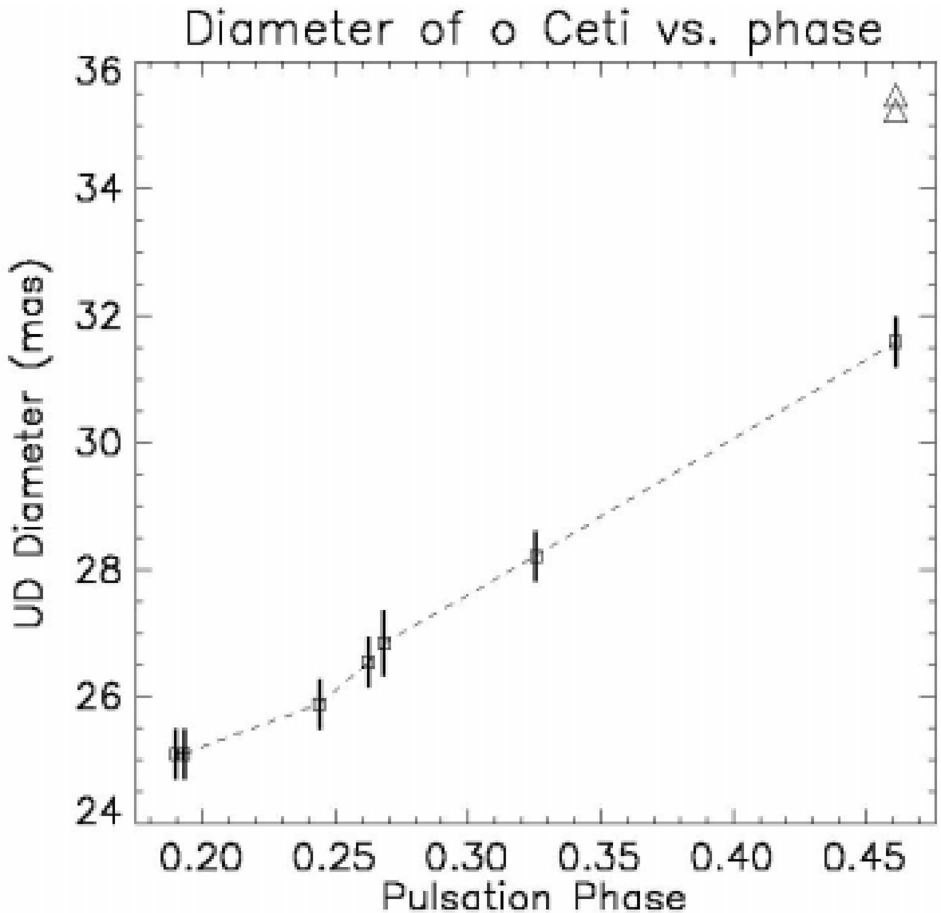

Using the 2-parameter model (proper calibration of .60 and a varying diameter) here are the solved-for diameters as a function of Julian date. This plot was thrown in at the last moment because a disagreement had emerged at the conference over the *direction* of diameter variations over the star's pulsation cycle. At K band according to this data (and according to additional near-IR and visible interferometric measurements) the diameter of the star is *increasing* during phase .2 - .45 at which time the luminosity of the star (especially in the visible!) is *falling*.

The anomolous result at 10 microns, a *decrease* in the star's diameter during these phases, might be explained by the 10 micron diameter being the result of circumstellar emission. When the luminosity of the star decreases, the radii at which various temperatures are found shrinks, and an "image" at that wavelength shows a decreasing size. Note that the 10 micron "diameters" of this star are almost twice as large as what is measured at near IR!

The End

We wish to acknowledge that data included herein is based on observations made with the European Southern Observatory telescopes obtained from the ESO/ST-ECF Science Archive Facility.